

NUMERICAL ANALYSIS OF BLAST  
PRESSURE PARAMETERS ON RC WALL  
WITH CIRCLE OPENING

MOHAMMAD FAZRIEL BIN ZAIDI

B. ENG (HONS.) CIVIL ENGINEERING

UNIVERSITI MALAYSIA PAHANG

## UNIVERSITI MALAYSIA PAHANG

### DECLARATION OF THESIS AND COPYRIGHT

Author's Full Name : MOHAMMAD FAZRIEL BIN ZAIDI

Date of Birth : 30<sup>th</sup> JUNE 1996

Title : NUMERICAL ANALYSIS OF BLAST PRESSURE  
PARAMETERS ON RC WALL WITH CIRCLE OPENING

Academic Session : SESSION II 2018/2019

I declare that this thesis is classified as:

- CONFIDENTIAL (Contains confidential information under the Official Secret Act 1997)\*
- RESTRICTED (Contains restricted information as specified by the organization where research was done)\*
- OPEN ACCESS I agree that my thesis to be published as online open access (Full Text)

I acknowledge that Universiti Malaysia Pahang reserves the following rights:

1. The Thesis is the Property of Universiti Malaysia Pahang
2. The Library of Universiti Malaysia Pahang has the right to make copies of the thesis for the purpose of research only.
3. The Library has the right to make copies of the thesis for academic exchange.

Certified by:

\_\_\_\_\_  
(Student's Signature)

\_\_\_\_\_  
(Supervisor's Signature)

960630-015601  
New IC/Passport Number  
Date: 17 June 2019

Dr. Mazlan Bin Abu Seman  
Name of Supervisor  
Date: 17 June 2019

NOTE : \* If the thesis is CONFIDENTIAL or RESTRICTED, please attach a thesis declaration letter.



## **STUDENT'S DECLARATION**

I hereby declare that the work in this thesis is based on my original work except for quotations and citations which have been duly acknowledged. I also declare that it has not been previously or concurrently submitted for any other degree at Universiti Malaysia Pahang or any other institutions.

---

(Student's Signature)

Full Name : MOHAMMAD FAZRIEL BIN ZAIDI

ID Number : AA15219

Date : 17 JUNE 2019

NUMERICAL ANALYSIS OF BLAST PRESSURE PARAMETERS ON RC  
WALL WITH CIRCLE OPENING

MOHAMMAD FAZRIEL BIN ZAIDI

Thesis submitted in fulfillment of the requirements  
for the award of the  
B. Eng (Hons.) in Civil Engineering

Faculty of Civil Engineering and Earth Resources  
UNIVERSITI MALAYSIA PAHANG

JUNE 2019

## ACKNOWLEDGEMENTS

In the name of Allah, the utmost grateful to Allah for His permission, that this thesis was successfully finished. Alhamdulillah, first and foremost, I would particularly like to express my deepest gratitude to Allah SWT for the guidance and help in giving me the strength to complete this dissertation.

I would like to thank you my family who have supported me while I have been completing my research in terms of moral and finance. Especially my parents, Zaidi bin Jusoh and Rosmah binti Hasan, who always give me a motivation and inspiration during my study and to my partner Muhammad Taufik bin Suhaimi who have always convinced me to complete my research.

In addition, I would like to express my sincere gratitude to my supervisor, Dr. Mazlan bin Abu Seman for the continuous support of my research, for his patience, motivation, enthusiasm, and immense knowledge. His guidance helped me in all the time of research and writing of this thesis. I am very fortunate to have benefited from the convergence of each of his unique expertise. The best parts of this thesis would not have been possible without his inputs.

And last, but not least, also the moral support of relatives and friends is important. However, I would like to particularly mention my research partner, Muhammad Taufik bin Suhaimi and my buddies Ahmad Ridhwan, Mohd Zarif, Ahmad Fathiey and Muhammad Nur Aiman who have provided extraordinary moral support to ease my countless episodes of sufferings throughout the process.

## ABSTRAK

Dinding konkrit bertetulang dikenali sebagai dinding penghalang yang digunakan untuk melindungi bangunan atau kawasan dari beban letupan. Dinding konkrit bertetulang adalah jenis yang digunakan untuk perlindungan. Kajian lanjut diperlukan untuk menyiasat letupan beban tekanan lampau kerana letupan dengan berat badan setara 13.61 kg (30 paun) TNT di kawasan medan letupan. Kerja sekarang bertujuan untuk menentukan kesan pada ubahan tekanan letupan disebabkan oleh dinding konkrit bertetulang dan dinding konkrit bertetulang dengan pembukaan bulatan jarak jarak jauh 1219 mm dari pusat berat caj sebagai jisim Trinitrotoluene (TNT) bersamaan dengan menggunakan perisian Analysis Unsur Terhingga, AUTODYN. Dinding konkrit bertetulang mempunyai dimensi keratan rentas 1829 mm x 1219 mm dengan ketebalan dinding 152 mm dan tebal 305 mm tapak kaki. Analisis letupan beban tekanan lampau dibahagikan kepada empat bahagian. Bahagian pertama menunjukkan analisis beban tekanan lampau ledakan berat 13.61 kg (30 paun) TNT dengan berat caj di tempat berlokasi 5486 mm (18 kaki) di ruang bebas. Berat caj terletak pada jarak 1219 mm (4 kaki) dari pusat dinding konkrit bertetulang. Kajian ini membandingkan ubahan beban tekanan lampau seperti yang dilaporkan oleh Yan et al. (2011) daripada ubahan letupan beban tekanan lampau. Bahagian kedua membentangkan analisis beban tekanan lampau ledakan 13.61 kg (30 paun) berat caj TNT yang terletak pada 1219 mm (4 kaki) dari dinding konkrit bertetulang. Tolok tekanan terletak pada 1219 mm (4 kaki), 2438 mm (8 kaki.), 3657 mm (12 kaki.), 4876 mm (16 kaki.) dan 5486 mm (18 kaki) . Bahagian ketiga menunjukkan analisis beban tekanan lampau ledakan 13.61 kg (30 paun) TNT berat yang terletak pada jarak 1219 mm (4 kaki) dari dinding konkrit bertetulang dengan 25% pembukaan bulatan manakala bahagian keempat juga sama dengan bahagian ketiga tetapi digantikan dengan dinding konkrit bertetulang dengan 50% pembukaan bulatan. Tolok tekanan berdasarkan bahagian kedua dan ketiga terletak sama berdasarkan lokasi tolok tekanan dari bahagian kedua. Dari hasil analisis letupan beban tekanan lampau, tekanan beban tekanan lampau antara dinding konkrit bertetulang (Jenis 2), dinding konkrit bertetulang dengan 25% pembukaan bulatan (Jenis 3) dan dinding konkrit bertetulang dengan 50% pembukaan bulatan (Jenis 4) adalah sama dalam jangka masa ubahan tekanan letupan. Ia adalah kerana jenis dinding konkrit bertetulang mempunyai kriteria dan sifat yang sama. Oleh itu, dinding konkrit bertetulang adalah mungkin untuk menggantikan dengan dinding konkrit bertetulang dengan pembukaan bulatan (25% atau 50%) kerana ia dapat menjimatkan kos peratusan konkrit tetapi tetap sama dalam jangka masa ubahan tekanan letupan. Dinding konkrit bertetulang dengan pembukaan bulatan memberikan lebih banyak nilai estetik dan ekonomik untuk menjadi perlindungan dalam jangka masa ubahan tekanan letupan. Dinding konkrit bertetulang juga mungkin menggunakan bentuk pembukaan lain seperti segi empat tepat, segi empat, segi tiga dan lain-lain yang akan memberi lebih berkesan dalam jangka masa ubahan tekanan letupan. Peratusan pembukaan yang digunakan untuk penyelidikan ini ialah 25% dan 50% pembukaan bulatan. Oleh itu, untuk penyelidikan seterusnya ia boleh mencadangkan dengan 30% atau 60% pembukaan bulatan untuk mendapatkan analisi yang lebih cekap berdasarkan letupan beban tekanan lampau.

## ABSTRACT

Reinforced concrete (RC) wall is known as barrier wall used to protect of buildings or areas from blast loads. RC wall is the type used for protection. Further study is needed to investigate blast overpressure due to the explosive with 13.61 kg (30 lbs.) TNT equivalent weight in blast field area. Present work aim to determine the effect on the blast pressure parameters due to the solid RC wall and solid RC wall with circle opening at 1219 mm standoff distance from the centre of the charge weight as an equivalent mass of Trinitrotoluene (TNT) by using Finite Element (FE) software, AUTODYN. The RC wall has a cross-sectional dimension of 1829 mm x 1219 mm with wall thickness of 152 mm and 305 mm thickness of strip footing. The blast overpressure analysis divided to four parts. The first part present the blast overpressure analysis of 13.61 kg (30 lbs.) TNT charge weight at located 5486 mm (18 ft.) away on the free-field space. The charge weight are located at 1219 mm (4 ft.) away from the centre of the RC solid wall. This research compared the blast overpressure parameters as reported by Yan et al. (2011) of the blast overpressure parameters. The second part present the blast overpressure analysis of 13.61 kg (30 lbs.) TNT charge weight located at 1219 mm (4 ft.) away from the RC solid wall. The pressure gauge are located at 1219 mm (4 ft.), 2438 mm (8 ft.), 3657 mm (12 ft.), 4876 mm (16 ft.) and 5486 mm (18 ft.) away from the charge weight. The third part shows the blast overpressure analysis of 13.61 kg (30 lbs.) TNT charge weight at located at 1219 mm (4 ft.) away from the RC wall with 25% of circle opening while fourth part also similar to the third part but replaced with RC solid wall with 50% of circle opening. The pressure gauge based on second and third part are located similarly based on the location of pressure gauge from second part. From the result of the blast overpressure analysis, the blast overpressure between RC solid wall (Type 2), RC solid wall with 25% of circle opening (Type 3) and RC solid wall with 50% of circle opening (Type 4) are similarly in the term of blast pressure parameters. It is because of the type of the RC wall have similar criteria and properties of the designation. Therefore, the RC solid wall are possible to replace with RC solid wall with circle opening (25% or 50%) because it can save the cost of the percentage of concrete but still with same in the term of blast pressure parameters. RC wall with circle opening give more aesthetic value and economical to be as protection in the term of blast pressure parameters. RC wall also possible to use another shape of opening such as rectangle, square, triangle and others that will give more effective in the term of blast pressure parameters. The percentage of opening that used for this research are 25% and 50% of circle opening. So, for next research it can suggested with 30% or 60% of circle opening to get more efficiently based on the blast overpressure analysis.

## TABLE OF CONTENT

<b>DECLARATION</b>	
<b>TITLE PAGE</b>	
<b>ACKNOWLEDGEMENTS</b>	<b>ii</b>
<b>ABSTRAK</b>	<b>iii</b>
<b>ABSTRACT</b>	<b>iv</b>
<b>TABLE OF CONTENT</b>	<b>v</b>
<b>LIST OF TABLES</b>	<b>viii</b>
<b>LIST OF FIGURES</b>	<b>ix</b>
<b>LIST OF SYMBOLS</b>	<b>xi</b>
<b>LIST OF ABBREVIATIONS</b>	<b>xii</b>
<b>CHAPTER 1 INTRODUCTION</b>	<b>1</b>
1.1 Research Background	1
1.2 Problem Statement	2
1.3 Objective of the Research	3
1.4 Scope of the Research	3
1.5 Significant of the Research	4
1.6 Outline of the Thesis	4
<b>CHAPTER 2 LITERATURE REVIEW</b>	<b>6</b>
2.1 Introduction	6
2.2 Blast Load	6
2.2.1 Explosions and Blast Phenomenon	12



2.2.2	Blast Load Characteristics	13
2.2.3	Blast Load Classification	15
2.2.4	TNT Equivalency	17
2.2.5	Blast Pressure Profile	17
2.2.6	Blast Wave Scaling Laws	19
2.2.7	Blast Interaction	20
2.3	Reinforced Concrete ( RC ) Wall	22
2.4	AUTODYN	27
2.4.1	Material Model for Concrete	27
2.4.2	Material Model for Steel Reinforcement	30
2.4.3	Material Model for Air and High Explosive	31
2.4.4	Erosion Model	31
2.5	Summary	32
<b>CHAPTER 3 METHODOLOGY</b>		<b>33</b>
3.1	Introduction	33
3.2	Numerical Modelling RC Wall Subjected to Blast Load in AUTODYN	34
3.2.1	Blast Overpressure Analysis	41
3.2.1.1	Air Volume Type 1	41
3.2.1.2	Air Volume Type 2	42
3.2.1.3	Air Volume Type 3	43
3.2.1.4	Air Volume Type 4	43
3.3	Summary	44
<b>CHAPTER 4 RESULTS AND DISCUSSION</b>		<b>45</b>
4.1	Introduction	45

4.2	Blast Overpressure Analysis in AUTODYN	45
4.2.1	Air Volume Type 1	45
4.2.2	Air Volume Type 2	46
4.2.3	Air Volume Type 3	48
4.2.4	Air Volume Type 4	49
4.3	Comparison of Peak Blast Overpressure between All Type of Air Volume	51
4.3.1	Type 2 with Type 3 of Blast Overpressure	51
4.3.2	Type 2 with Type 4 of Blast Overpressure	51
4.4	Summary	52
<b>CHAPTER 5 CONCLUSIONS AND RECOMMENDATIONS</b>		<b>53</b>
5.1	Conclusions	53
5.2	Recommendations	54
<b>REFERENCES</b>		<b>55</b>

## LIST OF TABLES

Table 2.1	Blast loading classification	15
Table 2.2	TNT Equivalent masses of some explosive	17
Table 3.1	Employed material data for concrete, input data to the RHT model	38
Table 3.2	Employed material data for steel reinforcement, input data to the JC model	39
Table 3.3	Employed material data for air, input data to the ideal gas EOS	40
Table 3.4	Employed material data for TNT, input data to the JWL EOS	41
Table 4.1	Comparison of peak blast overpressure-time history between Type 2 and Type 3	51
Table 4.2	Comparison of peak blast overpressure-time history between Type 2 and Type 4	52

## LIST OF FIGURES

Figure 1.1	Typical RC wall	1
Figure 1.2	Terrorist bombing attack in Bali	2
Figure 2.1	Blast wave diffraction over a barrier wall	10
Figure 2.2	Time arrival for blast wave fragments	11
Figure 2.3	Positive phase of the reflected blast wave	12
Figure 2.4	Blast wave propagation (Ngo et al., 2007)	13
Figure 2.5	Blast pressure vs duration behaviour (Magnusson, 2007)	14
Figure 2.6	Blast wave form surface burst	16
Figure 2.7	Typical blast pressure profile of a blast wave	19
Figure 2.8	Interaction of blast wave with an object with finite dimensions	21
Figure 2.9	Drag coefficients for a rectangular building subjected to explosive loading	22
Figure 2.10	Civil defence shelter and simplified model of one its walls	24
Figure 2.11	The concrete shear wall with opening (Semnan, 2011)	26
Figure 2.12	Maximum strength, yield strength and residual strength surfaces	28
Figure 2.13	Third invariant depend on stress $\pi$ plane	29
Figure 3.1	The flow chart of research framework	34
Figure 3.2	ALE solver technique in AUTODYN	34
Figure 3.3	Eight nodes hexahedral element	35
Figure 3.4	Detail of solid RC wall	36
Figure 3.5	Detail of RC wall with circle opening	36
Figure 3.6	Hexahedral meshing of RC wall	37
Figure 3.7	The 1m wedge (2D) filled with TNT and air	39
Figure 3.8	Pressure contours in 1m wedge (3D) during solving progress	40
Figure 3.9	Blast simulation in free-field	42
Figure 3.10	Blast simulation on solid RC wall	42
Figure 3.11	Blast simulation on solid RC wall with 25% of circle opening	43
Figure 3.12	Blast simulation on solid RC wall with 50% of circle opening	44
Figure 4.1	Comparison blast overpressure-time history	46
Figure 4.2	Blast overpressure-time history in Type 2	47
Figure 4.3	Blast vectors propagation of solid RC wall	47
Figure 4.4	Blast overpressure-time history in Type 3	48

Figure 4.5	Blast vectors propagation of solid RC wall with 25% of circle opening	49
Figure 4.6	Blast overpressure-time history in Type 4	50
Figure 4.7	Blast vectors propagation of solid RC wall with 50% of circle opening	50

## LIST OF SYMBOLS

kg	Kilogram
lbs	Pound
mm	Millimetre
ft	Foot
m	Metre
Pa	Pascal
ton	Tonne
cm	Centimetre
$\gamma$	Gamma
$\alpha$	Alpha
$\omega$	Omega
M	Mega
G	Giga

## LIST OF ABBREVIATIONS

RC	Reinforced Concrete
TNT	Trinitrotoluene
UFC	Unified Facilities Criteria
DOD	Department of Defense
ALE	Arbitrary Lagrange Euler
RHT	Riedel, Hiermayer and Thoma
JC	Johnson and Cook
JWL	Jones-Wilkins-Lee
EOS	Equation of State
FE	Finite Element
HOB	Height of Burst
2D	2 Dimension
3D	3 Dimension

# CHAPTER 1

## INTRODUCTION

### 1.1 Research Background

Concrete is widely used in construction as well as protective structure, due to its good energy absorbing characteristic under high pressures. Concrete has also been used in many constructions as walls because of the high quality, speedy construction, cost of construction and energy efficiency. In designing of the protective structures, it is important to follow the proper design standards or guidelines and also to identify the possible threats and their risk of occurrence to enable the characteristic of the design loads. The reinforced concrete (RC) wall used to protect buildings or areas from blast damage, highly combustible or explosive materials when exposed to the explosions. RC wall is the type used for wall protection. Figure 1.1 shows RC wall that used as the protection.



Figure 1.1 Typical RC wall

For example, the Oklahoma City Bombing was an assault that involved the bombing on the Alfred P. Murrah Federal Building on April 19, 1995. The blast damaged



324 buildings within 16 blocks and shattered glasses in and around 258 nearby buildings, causing at least an estimated, loss of \$652 million worth of damage. Figure 1.2 shows that the similar terrorist attack occurred in Bali bombing that happened on 12 October 2002 in the tourist region of Kuta on the Indonesian island of Bali. This terrorist attack led to improvements in engineering, especially in civil construction technology. This has allowed buildings to withstand greater forces, in which enhancements were incorporated into the design of new strong buildings.



Figure 1.2 Terrorist bombing attack in Bali

## 1.2 Problem Statement

In construction industry, blast impact study is very challenging due to the limitation to civilian and cost. The cost is very high due to the difficulty of the construction to build the building to resist blast load. Small RC panel subjected to blast load preferred in the experimental. Some researcher conduct blast test by validated 3D numerical modelling simulation. The result of the blast overpressure will approximately similar by validated numerical modelling vs experimental. This behaviour is similar to the numerical modelling research works conducted by Yan et al., (2011) and Seman, M. A. et al., (2019) where the simulated peak overpressure is close enough to the recorded blast overpressure, 490 kPa at 4.64 msec and 494.46 kPa at 4.62 msec, respectively.

Thus, insufficient study carried out for the RC wall subjected to blast load because of the limited access for civilian to conduct actual blast test. Nowadays, construction of

the structures are not designed to resist blast load and not enough knowledge or fact about the impact of the blast load if hit the structure and object nearby of it. The blast loading of structures behind a barrier wall (Zhou and Hou, 2006), study the empirical results of pressures on a rigid wall behind a barrier to predict peak reflected pressure and impulse. The studies based on barrier wall research that determine pressures on structures behind a blast wall. The barrier wall's effect on a blast wave without the interference of structures or how blast waves are affected by a barrier to cause loads on structures behind the barrier.

### **1.3 Objective of the Research**

The aim of this research is to investigate experimentally and numerically the behaviour of RC wall subjected to blast overpressure loading. To achieve this aim, specific objectives of the present work are set as follow:

1. The blast over pressure parameters of 13.61 kg (30 lbs.) TNT.
2. To study the blast overpressure parameters due to RC wall with and without circle opening.

### **1.4 Scope of the Research**

In order to establish the mentioned objectives of the present research, the scope of this research can be explained as follows:

1. The numerical modelling of 13.61 kg (30 lbs.) TNT in AUTODYN 3D Finite Element. The simulation of the result will be verified by blast overpressure from Yan et al. (2011).
2. The subsequent of the numerical investigation is based on the three sequence of the study, blast on solid RC wall, blast on RC wall with 25% of circle opening and blast on RC wall with 50% of circle opening.
3. The RC wall with circle opening subjected to blast load of 13.61 kg (30lbs.) TNT equivalent weight at 1219 mm away from wall of the centre (Yan et al., 2011) is considered by using numerical simulation, AUTODYN. The dimension of the RC wall is 1829 mm tall, 1219 mm

wide and 152.4 mm thick. The base of the wall is 1219 mm in square and 304.8 mm thick.

### **1.5 Significant of the Research**

The study is based on the 3D numerical model of blast that from AUTODYN. This study to compare the result that validated numerical modelling of 13.61 kg (30 lbs.) TNT for the pressure gauge at 5486 mm (18 ft.) from the charge weight versus experimental blast test that have been conducted by previous research Yan et., (2011). It is proved that the further parametric study can be carried out without additional cost. The study is possible to carry out since there is limited access for civilian to conduct actual blast test. Then, this research understanding the pressure parameter numerical modelling. The study shown that possible to design better RC wall to reduce cost but still valid as the protection wall barrier. The RC wall gives aesthetically value if it have different shape of opening or different of color and the RC wall not look as the war zone area. This will make the RC wall more attractive and give aesthetic value. Moreover, this study is helpful and useful to the construction industry and company professionals as most civilian infrastructure is not designed to resist the stress from the blast. These parties can introduce it in their training and in the region of development and construction management to a new invention or practice. In terms of taking precautionary steps against the disaster and unexpected events involving explosion, it will be helpful to consider blast stress on a structure and its surroundings. Furthermore, it is feasible to predict potential harm such as harm to infrastructure, injury to humans, and fatality with this research study on blast load impacts. This is due to the important numerical knowledge of the pressure parameters and the comparison of the literature review that offers more result on the behaviour of the blast pressure on different conditions.

### **1.6 Outline of the Thesis**

Thesis layout will summarize the details of the thesis. This thesis is organized into five chapters as detailed below:

Chapter 1 presents a general background and a discussion of the problem, the objectives, the scope of the research and as well as the significant of the research.

Chapter 2 presents the term of the blast load overview and its context, the RC subjected to blast load by considering the case study of investigation on 13.61 kg (30 lbs.) TNT and the numerical investigation of the blast load due to the RC wall based on references such as research articles, books, internet, and journals. For the current research, AUTODYN simulation package was used.

Chapter 3 describes the methods carried out for this research by using numerical simulation, AUTODYN. There are four categories of the impact due to the blast load, open field, RC solid wall, RC solid wall with 25% of circle opening and RC solid wall with 50% of circle opening.

Chapter 4 presents the blast overpressure analysis and numerical modelling of the blast overpressure impact on the RC wall according to the literature. The parametric results are established and are considered the subsequent analysis in the present research.

Chapter 5 summarized and discuss all the results based on the following blast overpressure analysis and give recommendation for the further research.

## **CHAPTER 2**

### **LITERATURE REVIEW**

#### **2.1 Introduction**

This chapter presents the three topics covered in this research, the term of the blast load overview and its context, the RC wall subjected to the blast load and the numerical investigation of the blast load to the RC wall. The sub section of the blast load classification can be divided based on either unconfined or confined explosion containment of the explosive charge. Then, the sub section under TNT equivalency describes the blast wave parameters and the detonation characteristics of each type of explosive material. The numerical investigation sub section focuses on the use of the commercial software AUTODYN.

#### **2.2 Blast Load**

For many years, structures have undergone blast loads due to large-scale blasts. The causes of these large-scale blasts were devices ranging from terrorist devices and conventional explosive charges to nuclear weapons. For example, 5.5 tons of explosives in a vehicle bomb were detonated at the U.S Marine Corps Battalion Headquarters in Beirut in 1983. From the incident, over 300 people were killed or wounded in the attack, which demolished the concrete building in contact with the vehicle. Then, 2.8 tons of explosives were used to attack the U.S Embassy Annex in 1984 at Antilias. From the case, the car bomb was detonated on a sunken road approaching the Annex car park and small retaining all provided some shielding to the blast at a standoff distance from the embassy. The casualty rate was relatively low due to the barrier wall and there were only 11 deaths recorded (Smith and Hetherington, 1994). This situation give some ideas of how important blast barrier wall in the involving explosive attacks.

Blast loads have a peak pressure that decays exponentially over very short time duration (Baker, 1973) compared to that of common dynamic loading events such as wind loads. Blast pressure has a very high load, and is applied to a structure in a matter of only milliseconds. As the blast wave reflects away from the structure, it generates a vacuum that causes the air pressure to drop below that of the ambient air pressure. This is called the negative phase of a blast. The area under the pressure–time history curve is called the impulse and is a measure of the energy imparted to the structural components.

Generally, when a blast event occurs, the exterior walls of a structure are subjected to direct, reflected pressures from the blast. The high explosives result in high overpressures of a very short duration. As a consequence, such explosions lead to highly dynamic loadings on reinforced concrete walls and structures. The overpressures, as a result of the shock wave, will propagate through the atmosphere and arrive at the target structure. The fragments generated by the explosion and the shock loads produced by the energy of the detonation can cause damage to walls and structures. The damage level experienced by walls subjected to blast loading can be severe. Therefore, it is of interest to understand the behaviour of the RC walls under blast loading.

The two key blast parameters that most directly impact the blast environment are the explosive weight or charge weight and the stand-off distance between the blast source and the target structure. In a design or analysis procedure, the characteristics of the dynamic loading, in terms of pressure and impulse, are determined by these two parameters. Given that full-scale testing of realistic explosive effects is economically not viable and time consuming, small-scale experimental testing is accepted as a well-proven alternative to assess blast loading. This is possible since many blast parameters can be scaled for charge masses ranging from milligrams to tons. The most widely used method of blast scaling is on the basis of the Crank-Hopkinson's "cube-root" law for scaled distance, time and impulse (Loiseau et al., 2008). All blast parameters such as peak pressure, time and impulse are primarily dependent on the amount of energy released by a detonation of charge in the form of a blast wave and the distance from the explosion. The Hopkinson-Cranz law provides a universal normalized description of the blast effects in terms of scaled distance, where the scaled distance is based on a constant of proportionality between stand-off distances and charge weights that result in the same

incident pressures. The Hopkinson-Cranz law permits experimental testing over very wide ranges of explosive energies and distances, including very strong shock conditions.

Explosive loads have received considerable attention in recent years due to a variety of accidental or intentional events that have affected major structures and their occupants worldwide the worst. Structures normally are not designed to resist blast loads because the construction of the structures is very high. The magnitude of design loads is significantly lower than most explosions, and conventional structures are susceptible to damage from such attacks.

Explosive threats can be detonated within a close range of a target, resulting in high pressure loads and flying debris that can cause severe personal and structural damage. One of the most significant attacks was that which took place in Saudi Arabia in the city of Al-Khobar in June 1996 (Crowder et al., 2004). The bomb caused an extensive damage to one of the building towers. According to Saudi and Pakistani press accounts, al-Mughassil was found in Beirut and has been transferred to the kingdom. Nineteen United States Air Force personnel were killed at Khobar and 372 wounded by the attack. The timing of the capture will raise questions about how it might impact the Iran nuclear deal debate.

Structures around the world are increasingly exposed to the threat of terrorist attacks and other forms of explosion. The US state department in its 2012 annual report on terrorism reported a total of 6,771 terrorist attacks worldwide resulting in as many as 11,000 deaths and more than 21,600 injuries (U.S. Department of State, 2013). In 2013, there was a 43% rise in global terrorism, as the US state department reported 9,707 terrorists' attacks, with over 17,800 deaths and more than 32,500 injuries (U.S. Department of State, 2014). This alarming trend must be addressed through sophisticated security protocols and blast hardening to protect citizens. When the security protocols fail, the blast hardened structure is expected to resist the abnormal blast loads and protect the building occupants while limiting structural damage to the expected performance level.

A bomb blast inside of a building can cause catastrophic destruction of the external and internal structural frameworks of the building, weaken the wall structure, blow out large window spaces, and shut down critical life-safety systems. Loss of life

and injury to occupants may result from numerous causes, including direct blast effects, structural collapse, impact of debris, fire, and smoke. Blast destructive evaluation of buildings and structural elements requires precise prediction of blast loads in terms of peak pressures and impulses. Using empirical relationships, blast loadings on structures were typically evaluated. These relationships assume that between the explosive device and the target there are no obstacles. For some distance behind the barrier, if a blast barrier is used to protect personnel or a structure behind it, the actual blast loading environment will be reduced.

According to Nathan Thomas (2010), to understand how a wave of blast pressure interacts with a barrier wall, a free-field blast pressure wave must first be understood. The supersonic detonation within a high explosive forms gasses that are expanding violently. This expansion causes compression of the surrounding air layer and forms a blast wave. The blast wave that follows the detonation shock wave is a high pressure wave front that expands out from the explosive charge. Before the air resumes its natural equilibrium at atmospheric pressure (Johansson and Persson, 1970 and Smith and Hetherington, 1994), a negative pressure trough follows.

The blast wave propagates along the surface until it is no longer supersonic when apply in a free-field area. The barrier wall simulates a blast interaction with a large target. The blast wave from a charge at some standoff distance impacts the barrier wall based on its size. This causes the blast wave to diffract over the barrier wall as shown in Figure 2.1. Before that distance becomes large enough that the pressure is no longer affected by the wall, the wave is reduced for some distance behind the barrier wall (Smith and Hetherington, 1994 and Remennikov and Rose, 2007). The area where the wall affects the blast pressures and causes a pressure reduction that defined as the shadow area. The extent of this shadow area defines the barrier wall's effectiveness in reducing pressure.



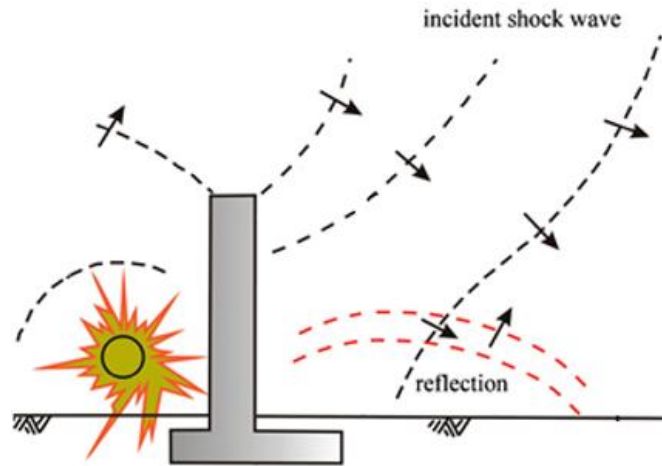


Figure 2.1 Blast wave diffraction over a barrier wall  
 Source : Remennikov and Rose (2007)

The research of Remennikov and Rose (2007) explain that the use of empirical data and neural networks to predict the area of the blast barrier wall effect on structures behind a wall. It investigates that how a blast wave is affected by a barrier wall and examined the physical changes. Zhou and Hao (2006) also describe the blast loading of structures behind a barrier wall. The study of the research is to know the result of pressures on a rigid wall behind a barrier to predict peak reflected pressure and impulse. Most of studies are based on barrier wall research that determine structural pressures behind a blast wall. However, they also study the effect of the barrier wall on the blast wave without structural interference or how the blast waves are affected by the barrier causing loads on the barrier structures. Studying the effect of a barrier wall on a blast wave would help to fully understand the area of pressure reduction due to a barrier wall and how the blast pressure on the horizontal plane is affected by a barrier wall.

Walter (2004) describes the process of measuring air blasts and details how to properly use a pressure transducer. The article study on how an explosive waveform progresses and show the difference between incident pressure, free-field pressure, and reflected pressure. It explains the synonymous incident pressure and free-field pressure and describes the pressure created by an expanding shock wave. It creates a reflected pressure wave when the free-field wave reflects from a surface. Side-on transducers are used to measure free-field pressures without interfering with the flow behind the shock wave, while reflected-pressure transducers are used to measure reflected pressures on a rigid surface at normal incidence.

As Ulrika Nystrom et al., (2009) carried out the studies, as detonation of the explosive filler in a cased bomb is initiated, the inside temperature and pressure will increase rapidly and the casing will expand until it breaks up in fragments. The remaining energy after swelling and fragmentation of the casing will giving the fragments velocity expands into the surrounding air then it will creating a blast wave. There are at least three types of loading effects must be considered when the structures around a bomb detonation that exposed to both blast and fragment loading. The three types of loading effects must be considered that is impulse load from blast wave, impulse load from striking fragments and impact load from striking fragments. The impulse is considered to give a global response and impact a local response caused by the penetration of the fragments.

Since the properties of bomb and its position relative to target and the surrounding environment have influence on the loading conditions, all these parameters will be considered during analysis of the loading effect. The distance from the detonation will greatly influence the loading properties. This cause by the change in peak pressure for the blast wave and the change in velocity of the fragments, which both decrease with increasing distance. For a 250 kg general purpose bomb (GP-bomb) with 50 weight per cent TNT, the blast front and the fragments will strike the target at the same time at an approximate distance of 5 m. Figure 2.2 shows the time of arrival for blast wave and fragments as function of the stand-off for a 250 kg GP bomb with 50 weight per cent TNT.

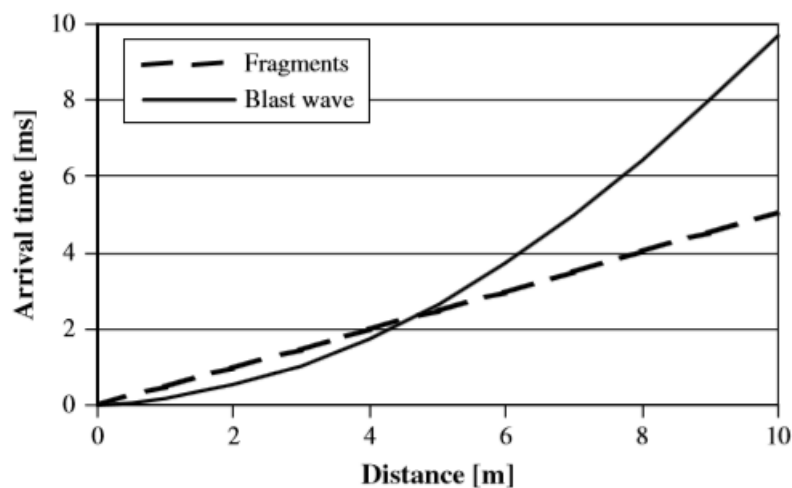


Figure 2.2 Time arrival for blast wave fragments  
Source : Ulrika Nystrom et al. (2009)

Figure 2.3 shows the positive phase of the reflected and incident blast wave for 125 kg TNT at 5 m stand-off. As the blast wave strikes a wall, it is reflected and its behaviour changes. The behaviour called as normal reflection that taking place as the blast wave is reflected against a perpendicular surface. For case charges the blast load characteristics depend not only on the type and amount of explosive and the stand-off distance, but also on the properties of the casing. An expression for calculating an equivalent uncased charge weight is given as a function of the ratio between the casing weight and the actual charge weight.

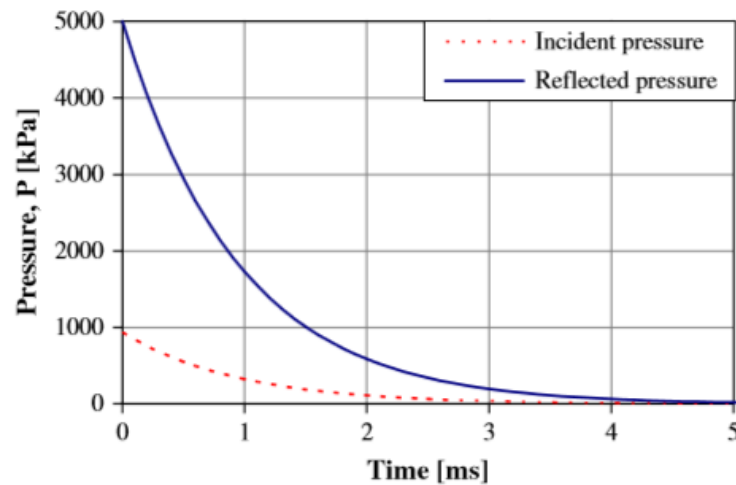


Figure 2.3 Positive phase of the reflected blast wave  
Source : Ulrika Nystrom et al. (2009)

### 2.2.1 Explosions and Blast Phenomenon

An explosion is defined as a large-scale, rapid and sudden release of energy. The detonation of the explosive generates a significant amount of energy, which causes the explosive gas to expand forcing the surrounding air out of the space. A compressed layer of this air known as shock front, is formed at the instant of the detonation. It contains most of the energy released from the explosion and expands outwards at supersonic speed. As the blast wave propagates, it decreases in strength, extends in duration and decreases in the velocity and temperature of the front shock and propagates quickly from the source of blast.

For the purpose of designing protective structures to resist the effects of blast loading, blast pressures and fragments generated by the explosion and the shock loads produced by the shock wave transmitted through the air or ground are the main explosion

effects to be considered (Magnusson 2007). Based on these three parameters, the blast pressures are usually the governing factor in determining structural response. Detonation produces an overpressure peak. Thereafter, as the blast wave propagates outward from the explosion source to the sounding air, the pressure decreases and drops. The blast wave is characterized by a sudden increase in pressure to a value above ambient atmospheric, followed by a decrease to an atmospheric pressure. This duration is referred to as the positive phase. After a short period of time, the pressure behind the shock front falls below the atmospheric pressure that known as negative phase. The variation of blast wave pressure with distance from explosion is presented in Figure 2.4.

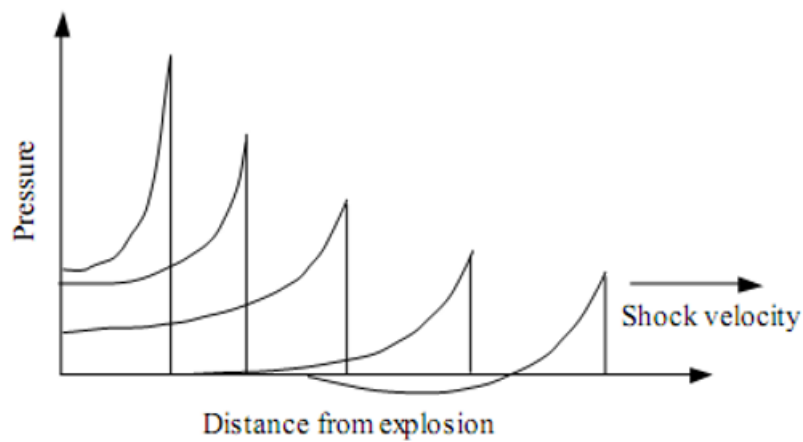


Figure 2.4 Blast wave propagation  
Source : Ngo et al. (2007)

### 2.2.2 Blast Load Characteristics

To study the blast effects on a given structure, the characteristics of the blast wave must be known. The explosive wave is characterized by a sudden increase in pressure to peak, followed by a decrease to an atmospheric pressure (positive phase), and then a further decrease in pressure below the atmospheric pressure (negative phase). The typical pressure-time history of the blast waveform generated by a free-air detonation from an explosive at some stand-off distance is given in Figure 2.5.

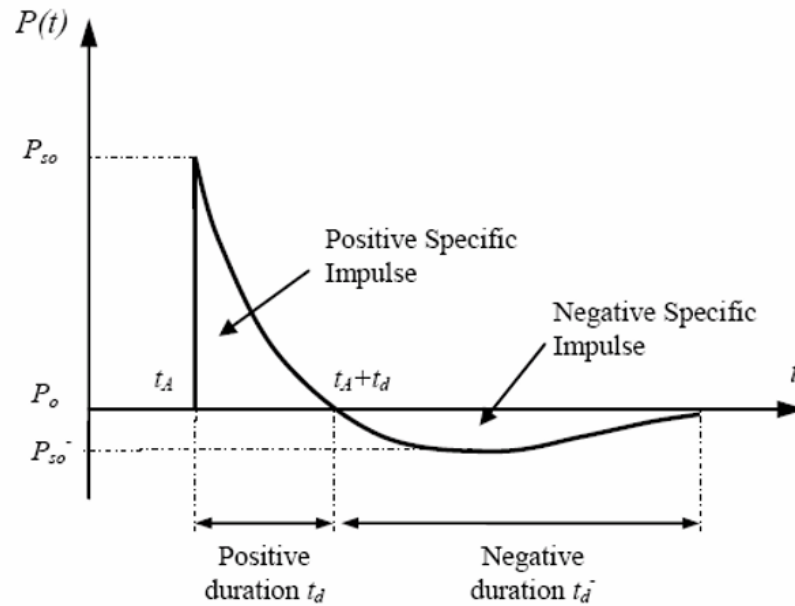


Figure 2.5 Blast pressure vs duration behaviour  
Source : Magnusson (2007)

The main characteristics of the development of this pressure wave are these following, the arrival time of the blast wave, the peak overpressure, the ambient pressure, the positive phase duration time, the maximum negative pressure, and the duration of the negative phase. The positive impulse is determined from the area bounded by the peak overpressure and the positive phase duration. At the arrival time of the blast wave the pressure suddenly increases in an extremely short rise-time to attain its peak overpressure over the ambient pressure. The pressure then starts decreasing until it reaches the ambient pressure at time. After this point, the pressure decays below the ambient pressure until it reaches the maximum negative pressure and then eventually returns to ambient condition in the duration of the negative phase denoted.

The blast shock wave propagates as a sphere of compressed gas that rapidly moves outwards from the explosive source. When the incident pressure wave impinges on a surface of a structure that is not parallel to the projection of the shock wave, the pressure is reflected and increasing in magnitude, producing what is known as the reflected pressure. The reflected pressure is always greater than the incident pressure for the same distance from the explosion. Ngo et al., (2007) stated that when the shock wave encounters any structure in its path, the incident peak overpressure is magnified by a reflection factor that depends on the intensity of the shock wave.

### 2.2.3 Blast Load Classification

Blast loads on structures can be divided based on either unconfined or confined explosion containment of the explosive charge, according to the Unified Facilities Criteria (UFC) (DOD, 2008). It could be divided based on the blast loading produced within the structure or acting on structures. Table 2.1 shows the blast loading categories with five possible pressure loads that related with respective categories. The problem is classified as unconfined explosion and categorised as a surface burst. If an explosion occurs in free air adjacent to and above building structures, an initial shock wave is produced without amplifying its wave between the explosive charge and the structures, then the explosive loads on the structures are known as the explosion of free air burst. The ground reflection of the initial wave occurs for this type of explosion before the blast wave arrives at the structure. UFC stated that An explosion in the air burst is limited to an explosion occurring two to three times the height of one or two storey building. If the explosion load charge is located near or on the ground surface, the initial shock wave is amplified by ground reflection at the point of detonation and then it will be considered as surface burst (Remennikov and Rose, 2007, and DOD, 2008).

Table 2.1 Blast loading classification

<b>Charge Confinement</b>	<b>Category</b>	<b>Pressure Loads</b>
Unconfined explosion	1. Free Air Burst	a. Unreflected
	2. Air Burst	b. Reflected
	3. Surface Burst	c. Reflected
Confined explosion	4. Fully Vented	c. Internal Shock d. Leakage
	5. Partially Confined	c. Internal Shock e. Internal Gas d. Leakage
	6. Fully Confined	c. Internal Shock e. Internal Gas

Source : DOD (2008)

The radially propagating blast wave between the explosive charge and structure is amplified when an explosion occurs without obstructions in the air medium. The blast load on the structure is known as the free air explosion. Based on (DOD, 2008), the distance from the explosive centre above the ground is usually about two to three times the structure height. An explosion of air caused by the explosive above the ground and at a distance from the structure, the initial blast wave, propagates and affects the surface of the ground before arriving at the structure. The blast considered as surface explosion

when the explosive charge is located above the ground at the height of burst (HOB) within 1 to 2 m. The ground surface reflected and amplified the initial incident blast waves of the explosion to produce a reflected blast wave. Thus, the front of the blast wave is a hemispheric blast wave propagating towards the target.

Uddin et al., (2010) has stated that the blast surface explosion is different from an air explosion, where the incident and reflected blast wave merge instantly as shown in Figure 2.6. There will be a single shock front at successive times  $t_1$  through  $t_4$  in a hemispheric form. The shock front will essentially vertical when the surface is close, and the dynamic wind behind the front will blow in horizontal direction. Then, the loads produced by overpressure and dynamic pressures are more critical than loads of a similar type at a high intensity and relatively short duration. The combination of blast pressures results in heavy transient loads on the structures, suggesting that the structural design requires dynamic analysis.

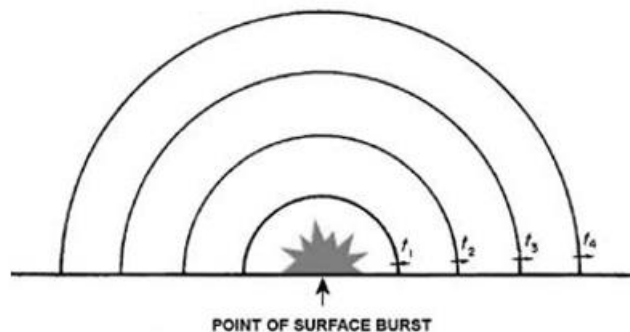


Figure 2.6 Blast wave form surface burst  
Source : Uddin et al. (2010)

In addition, when the ground surface were a perfect reflective surface, the surface explosive load weight would effectively double. However, a multiplier of approximately 1.7-1.8 is incorporated due to the energy dissipated in the production of a ground crater and ground shock (Uddin et al., 2010). When an explosion occurs with an obstruction of the propagating blast wave such as wall structure, as the blast wave strikes the wall surface at a normal angle of incidence ( $\alpha$ ), the overpressure incident is magnified due to the propagation of the blast wave through the suddenly arrested air and redirected by the wall surface.

## 2.2.4 TNT Equivalency

Trinitrotoluene (TNT) is the generally accepted standard. It is a relatively pure, safe to handle, and readily available explosive. To quantify and determine the blast wave parameters and evaluate the detonation characteristics of each type of explosive material, a datum is required. There has been a lot of research and testing using TNT. The majority of data on blast effects and blast pressure output from a spherical TNT explosive charge (Beshara, 1994). In quantifying a blast wave from a source other than TNT, the first step is to convert the charge mass into an equivalent mass of TNT (Braithwaite, 2012). This is done so that the explosive's charge mass is multiplied by the conversion factor based on the charge's and TNT's specific detonation heat. It should be noted that, the equivalency of materials compared to TNT may be affected by other factors such as material shape, the number of explosive items, explosive confinement, nature of source and the pressure range being considered (Beshara, 1994).

Table 2.2 TNT Equivalent masses of some explosive

Explosive	Density (kg/m <sup>3</sup> )	TNT Equivalence Mass for Pressure	TNT Equivalence Mass for Impulse
Amatol	1590	0.97	0.87
ANFO (94/6 ANFO)	800	0.87	0.87
Composition C4	1590	1.20	1.19
HMX	1910	1.25	1.25
PETN	1770	1.27	1.27
RDX	1820	1.10	1.10
TNT	1630	1.00	1.00
Tritonal	1720	1.07	0.96

Source : Braithwaite (2011)

## 2.2.5 Blast Pressure Profile

According to Farouk Siba (2014), when an explosive is detonated, large amount of energy is generated. This energy forces the explosive gas to expand and move outward from the detonation centre resulting in a compressed air layer called the blast wave. As the shockwave expands, the incident or overpressure decreases. Based on Hinman (2003), when it finds a surface denser than the medium in which the shockwave propagates, it is reflected resulting in a tremendous pressure amplification. The article explained that unlike acoustical waves which reflect with an amplification factor of two, shockwaves can reflect with an amplification factor of up to twelve, due to the supersonic velocity of



the shock wave at impact. The magnitude of the amplification factor is a function of the proximity of the explosion and the angle of incidence of the shockwave on the surface.

The reflected blast waves are categorized into three types that is normal, oblique and Mach reflection (Braithwaite, 2012). A normal reflection occurs when the blast wave impinges normally on an infinite reflecting surface. When the blast wave impinges on a reflecting surface at an incidence angle less than 90°, an oblique reflection occurs (Braithwaite, 2012; Hornung, 1986). When the expanding shockwave is reflected off the ground to form a second wave that travels behind the expanding shock wave, Mach stem reflection occurs. This reflected wave travels faster than the expanding shockwave, since it is traveling through a pre-compressed fluid. The reflected wave merges with the expanding shockwave to form a single wave called the Mach reflection or the Mach stem (Hornung, 1986; Hull, 1997). The peak pressure within the Mach stem regions can be twice as high as that of the original shock front (Hornung, 1986).

The pressure exponentially decays rapidly, measured typically in thousandths of a second. The partial vacuum leads to the formation of a negative pressure region behind the shock front thus creating a powerful wind or drag pressures (Hinman, 2003). The movement of blast wave in air is a nonlinear process involving a nonlinear equation of motion, whereas the wave propagation is a linear problem. Three primary independent parameters characterize the waveform. These parameters are the overpressure, the duration, and the impulse. The peak incident and reflected shockwave pressures and other useful parameters such as incident and reflected impulse, shock front velocity and time of arrival can be determined for an explosive threat defined by its load weight and standoff. Figure 2.7 presented the impulse of the blast wave is determined by calculating the area under a blast pressure-time profile.

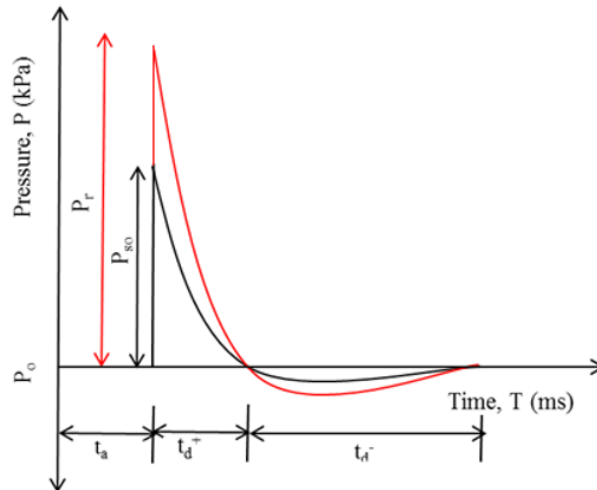


Figure 2.7 Typical blast pressure profile of a blast wave  
Source : Hinman (2003)

### 2.2.6 Blast Wave Scaling Laws

Blast parameters are primarily dependent on an explosive charge weight by a detonation in the form of a blast wave and the distance from the explosion. To characterize the properties of blast waves generated by explosives in free-air, extensive experiments have been conducted by researchers for many decades. The test results suggest that the blast waves follow scaling laws. Many blast wave parameters can be scaled for charge masses ranging from a few grams up to several tons.

The most common form of blast scaling is Hopkinson or ‘cube-root’ scaling law. The Hopkinson-Cranz law provides a universal normalized description of the blast effects in terms of scaled distance, where the scaled distance is the constant of proportionality between stand-off distances and charge weights that result in the same incident pressures. For example, two different weights of the same explosive detonated in similar atmospheric conditions, produce similar blast waves at some identical scaled distance. The scaled distance is an important parameter to determine the air-blast pressure and impulse. Other blast parameters can conveniently be plotted against the scaled distance. The Hopkinson-Cranz law is also useful for conducting experimental testing over a very wide range of explosive energies and distances, including very strong shock conditions. The usefulness is in the sense that the scaling law can be employed to find data for explosions to be tested in experiments to measure the properties of the blast wave.

In the study conducted by Luccioni et al. (2004), the Hopkinson-Cranz Scaling Law states that similar explosive waves are produced at identical scaled distances when two different charges of the same explosive and with the same geometry are detonated in the same atmosphere. Thus, any distance  $R$  from an explosive charge  $W$  could be transformed into a characteristics scaled distance:

$$Z = \frac{R}{W^{1/3}} \quad 2.1$$

where  $W$  is the charge mass expressed in kilograms of TNT. The use of  $Z$  allows a concise and efficient representation of blast wave parameters for a wide range of real situations. Huntington-Thresher and Cullis (2001) stated that different explosives are generally compared through their TNT equivalency both in terms of peak pressure and impulse. The TNT equivalency of an explosive is defined as the ratio of the mass of TNT to the mass of the explosive such that both result in the same magnitude of pressure or impulse.

Scaling laws provide parametric correlation relationships between a particular explosion and a standard charge of the same substance. The basic characteristics of the explosion and blast wave phenomena are presented together with a discussion of TNT equivalency and blast scaling laws. In general practice, prediction of blast pressure is based on scaled distance. All parameters of the pressure-time curve are also normally written in terms of a scaled distance.

### **2.2.7 Blast Interaction**

Once the blast wave is generated by the detonation of an explosive, it propagates away from the source at supersonic speeds, until it meets obstacles. When the blast wave encounters an object in its path, then reflection, refraction and diffraction occurs similar to a sound wave travelling through an air medium.

The occurrence of reflection, diffraction or refraction depends on the physical and geometrical properties of the obstruction. When the blast wave strikes perpendicular to the object, reflection occurs with increased pressure, density and temperature. The maximum increase of these parameters is observed when the obstruction has infinite dimensions perpendicular to the blast wave travel direction. These increases in physical parameters are directly due to the interaction of the original wave and the reflected wave.

The overpressure measured after the reflection is known as the *reflected overpressure* ( $P_r$ ), which is several times higher than the incident overpressure.

When the blast wave encounters a finite object in its path, diffraction may occur at the edges of the obstruction. In particular when a 3-dimensional object is exposed to blast waves, diffraction may reduce the effects of blast pressure on the side walls as shown in Figure 2.8. The front of the rectangular structure will encounter the maximum blast pressure while side walls and back wall will encounter much lower incident pressure.

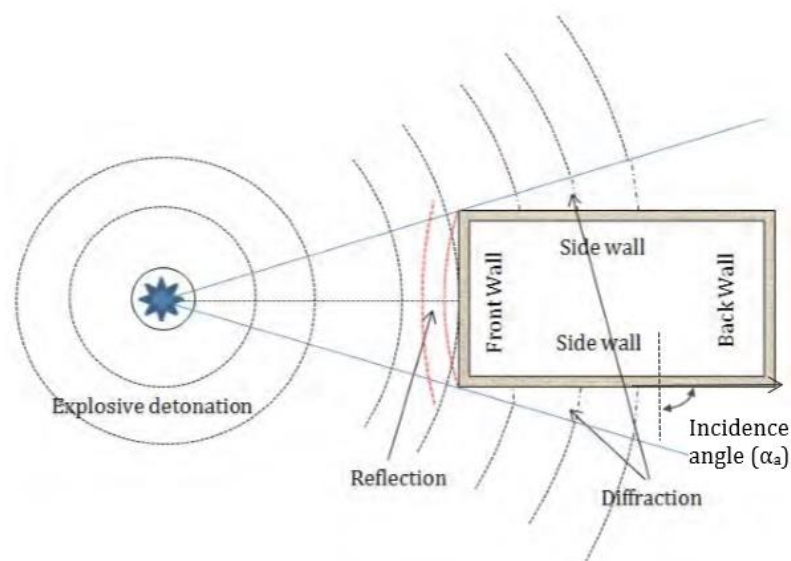


Figure 2.8 Interaction of blast wave with an object with finite dimensions  
Source : Ngo et al. (2007)

The magnification factor for the peak reflected pressure depends on the rigidity of the obstacle and incidence angle ( $\alpha_a$ ). The incident angle is defined as the angle between the blast wave propagation direction and the normal of the facing element of obstruction. When the obstruction is rigid and perpendicular to the blast wave, ( $\alpha_a = 0^\circ$ ), maximum magnification will occur and when the obstruction is parallel to blast wave ( $\alpha_a = 90^\circ$ ).

Reflection of blast waves can be classed either normal or Mach reflections (Anderson, 2001) depending on the incidence angle. Mach reflection is a supersonic shockwave effect observed when the shock wave propagates over a solid edge, which involves the formation of a triple point reflection. It has been found that Mach reflections

can occur only in the case of incident angle greater than  $40^\circ$  and when the incident angle is less than  $40^\circ$ , normal reflection will occur (Baker, 1973, cited in Ben-Dor, 2007).

The blast winds generated by the dynamic pressure also interact with the obstructions in its path in the same way as normal winds on structures, resulting in drag pressures. Drag pressures on a surface of an object depend on the dynamic pressure and the drag coefficient for that specific surface. Typical drag coefficients used for a rectangular structure are shown in Figure 2.9.

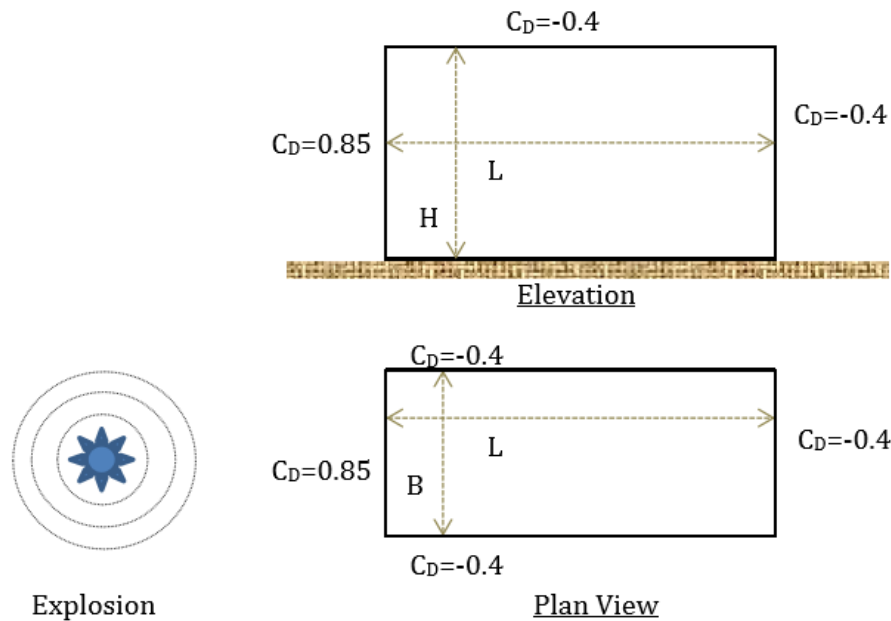


Figure 2.9 Drag coefficients for a rectangular building subjected to explosive loading

Source : Pham (2010)

### 2.3 Reinforced Concrete ( RC ) Wall

Reinforced concrete (RC) wall is widely used as construction material. The wall as barrier used to protect buildings or areas from blast loads. RC wall is the type used for the protection. Wall barrier can be used to mitigate explosive damage to target structures that would be harmed by a blast from the detonation of an explosive charge. The barrier walls serve to ensure that an explosive charge is set at a standoff distance away from a protected object. The barrier walls diffract blast waves to mitigate the full force of the blast pressures on the protected object. In the event of an explosion, a high level of energy from the explosive is transferred through the air in the form of a high-density shock wave.

This shock wave propagates through the atmosphere shocking the air with which it comes in contact along the way. The band of high-density air that defines the shock wave is compressed against the rigid surface when the shock wave impacts a rigid surface as it is forced to reflect off the surface. This reflection creates the peak reflected pressure load on the structure.

It is well known that the two most pronounced disadvantages of concrete are its low tensile strength and brittle behaviour. The tensile strength of normal strength concrete is less than one tenth of the compressive strength is reached, and then the tension strength is reached, the ability to transfer stresses through the material decreases rapidly. The brittle behaviour can also be seen in the case of uni-axial compression for high strength concrete, but the post fracture ductility in compression increases with a decreasing compressive strength. High dynamic loading giving a high strain rate in the material that also affect the strength and ductility of the concrete (Ulrika Nystrom et al., 2009).

Two separate experiments on blast load and single fragment impact were used to verify and calibrate numerical model. The validation and calibration process were done within a preliminary study and used to build up the numerical model of the wall strip subjected to blast and fragment impacts. Figure 2.10 shows the civil defence shelter is conceived as a reinforced that is solid concrete structure. For a shelter without backfilling the minimum thickness of the roof, walls and floor are specified as 350 mm, 350 mm and 200 mm, respectively while the concrete should fulfil a requirement of at least C25/30 according to (Boverket, 2004). A minimum reinforcement bar diameter of 10 mm and maximum bar spacing of 200 mm are required, with a maximum concrete cover of 50 mm.

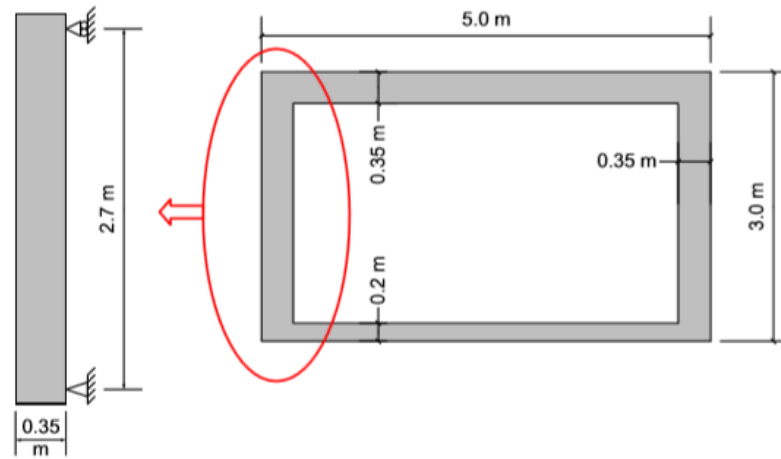


Figure 2.10 Civil defence shelter and simplified model of one its walls

Source : Boverket (2004)

The wall has a total height of 3 m and is simplified to be simply supported with a span length of 2.7 m. The rough simplification of the support conditions was not made in an attempt to imitate the real behaviour of the wall. (SRSA, 2009) explained that a static load of 50 KN/m<sup>2</sup> is used to calculate the required amount reinforcement in the walls, with a yield strength of 500 MPa were assumed and the distance form concrete edge to centre of reinforcement bars was chosen as 35 mm. The concrete was assumed to have a concrete strength of 35 MPa. The blast load is assumed to be uniform over the wall, which is reasonably accurate for the standoff distance (Johansson M., 2009).

E. Jacques (2011) studied the effect of retrofit techniques to improve the blast resistance of reinforced concrete RC walls and slabs. The research generate experimental data on the response of control and retrofitted RC panels subjected to shock waves and develop an analytical model to predict RC member response to blast loading. Y.S Tai et. al., (2011) explained that pressure-time history response to investigate the destructive effects on the RC slab subjected to the different amounts of explosives, different reinforcement ratios, and distance from the explosives. The analytical results demonstrated that bending damage or shear failure could occur at the center of the slab. The amount of explosive and distance from the explosion to the RC slab were cited to be important parameters. RC slab with low reinforcement ratio, damage was more probable at the centre of the slab. The slab deformation was reduced and damage was concentrated at the supports of the RC slab with the increased reinforcement ratio.

Y. Shi et al., (2010) has stated that the prediction of the structural frame collapse process responding to blast loading from the proposed method was similar to the prediction generated from the numerical simulation by directly applying the blast loads on the structural frame. The proposed method incorporating non-zero initial conditions and initial damage to adjacent structural members under blast loading was efficient and reliable in simulating the progressive collapse process of RC frame structures. The method that is including non-zero initial conditions and initial damage to adjacent structural members under blast loading would significantly reduce comprehensive computations compared to the direct numerical simulation approach.

The performance of exterior RC walls under different blast loading due to a terrorist event numerically and experimentally. The calibrated numerical model was then utilized to simulate the response of a typical exterior RC wall under blast loadings arising from terrorist bombings. Two parameters in this studied included charge weights (TNT equivalent) and the stand-off distance. The selected TNT charge weights corresponded to typical terrorist bombs. Four concrete damage categories under blast loading were considered, no damage, slight damage, moderate damage and severe damage. The numerical model was reasonable predictions of exterior RC wall response subjected to blast loading in the event of terrorist bombing.

In the study of Bao and Lio (2010), the researchers conducted the numerical simulation to evaluate the dynamic response of columns subjected to blast loadings. Bao and Lio state that the most of terrorist attacks on public structures were explosions at a short standoff distance that less than 10 m. Then, they use 5 m for their standoff distance and considering the limitation of the weight of explosives that can be obtained at a particular location that is a maximum TNT equivalent charge mass of 907 kg (1 ton) was used in this numerical simulations. They concluded that seismic detailing significantly reduced the degree of blast induced damage and subsequent collapse of reinforced concrete columns.

Hui and Bing (2003) have modelled a coupled shear wall under lateral load. Experimental analysis has shown a considerable increase in lateral strength with diagonal tensile tie and compressive strut. In another research, two concrete shear walls with opening have been assessed by Doh and Fragomeni (2004). This coupled shear walls



were 120 x 120 x 10 cm, with an opening with dimensions 30 x 30 cm. This study has been carried out to find a better behaviour for shear walls.

Kheyroddin and Naderpour (2008) retrofitted the link beam in coupled shear walls using CFRP, they indicated a statistical method to increase the strength and ductility of the shear wall. Khatami (2010) studied coupled shear walls under cyclic loading and recommended optimization side for openings on concrete shear walls. Barjari (2012) investigated coupled shear walls that have been retrofitted. The effect of steel reinforcing plates was seen to significantly increase the ultimate strength of coupled shear walls.

Seyed et al., (2012) has investigate two different types of openings. Results of three buildings with coupled shear wall, rectangular shear wall and square shear wall are compared in this investigation. All the models have been analyzed under lateral time history, lateral displacements, energy absorption capacity and hysteretic behaviours have also been determined. In the first study, the complete shear wall of the 3D building was able to absorb more energy than other investigated models of shear wall with openings. As opening decreases lateral carrying capacities of shear walls and panels, the second study also indicated a deformation delay of the panel with opening as compared with the complete panel occurring at the yielding load level. These facts are characteristic of the behavior and performance of shear walls and panel with openings, decreasing their role in lateral load carrying capacity. Figure 2.11 show the concrete shear wall with opening (Semnan, 2011).



Figure 2.11 The concrete shear wall with opening  
Source : Semnan (2011)

## 2.4 AUTODYN

Based on previous research by Tu and Lu (2009), Nystrom and Gylltoft (2009), Kamal and Eltehwewy (2012) and Wang et al. (2013), the standard material for concrete and steel in AUTODYN such as CONC-35MPA and STEEL 4340 is assigned. The material for concrete and steel is based respectively on the material model of Riedel, Hiermayer and Thoma (RHT) and the material model of Johnson-Cook (JC).

However, the Piecewise Johnson-Cook is used to describe steel behaviour (Nystrom and Gylltoft, 2009) and the modified parameter RHT is used to describe concrete behaviour (Tu and Lu, 2009) to provide accurate approximation by parameter in each research work conducted.

### 2.4.1 Material Model for Concrete

A proper model that reflects concrete material behavior at a high strain rate is vital to obtain a reliable prediction of concrete behavior under blast loads. The material model developed by Riedel, Hiermayer and Thoma (RHT) is adopted in this study (Riedel et al., 1999). The RHT concrete model is an advanced plasticity model for brittle materials. It is useful for modelling the dynamic loading of concrete. The model includes pressure hardening, strain hardening, strain hardening, third invariant compressive and tensile meridian dependency, and strain softening damage model. This model also uses the  $p - \alpha$  state equation (Herrman, 1969) to represent high stress concrete thermodynamic behaviour, providing a reasonably detailed description of compaction behaviour at low stress ranges. It is established that at the same pressure and temperature the specific internal energy for the porous material is the same as the solid material. The model consists of three pressure-dependent surfaces, a fracture surface, an elastic limit surface, and the crushed material's residual strength surface. Figure 2.12 shows these strength surfaces.

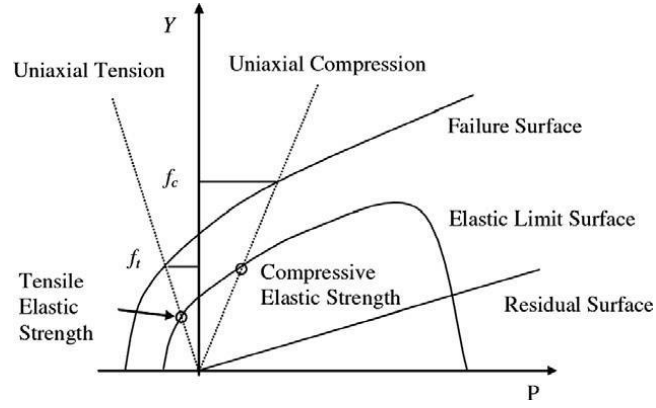


Figure 2.12 Maximum strength, yield strength and residual strength surfaces  
Source : ANSYS (2019)

The failure surface,  $Y_{fail}$  is defined as a function of the normalised pressure  $p^*$ , lode angle  $\theta$  and strain rate  $\dot{\epsilon}$ :

$$Y_{fail}(p^*, \theta, \dot{\epsilon}) = Y_c(p^*) \cdot r_3(\theta) \cdot F_{rate}(\dot{\epsilon}) \quad 2.2$$

Where  $Y_c(p^*)$  is the comprehensive meridian and it is represents by

$$Y_c(p^*) = f_c \left[ A \cdot \left( p^* - p^*_{spall} F_{rate}(\dot{\epsilon}) \right)^N \right] \quad 2.3$$

Where,  $f_c$  denotes the material uniaxial compressive strength;  $A$  is failure surface constant;  $N$  is failure surface exponent;  $p^* = p / f_c$  is normalised pressure; and  $p^*_{spall} = f_t / f_c$ , where  $f_t$  is the material uniaxial tensile strength;  $F_{rate}(\dot{\epsilon})$  represents the dynamic increase factor (DIF) as a function of strain rate  $\dot{\epsilon}$ .  $r_3(\theta)$  defines the third invariant dependence of the model as a function of the second and thrid stress invariant and a ratio of strength at zero pressure  $Q_2$ . Figure 2.13 illustrates the tensile and comprehensive meridian on the stress  $\pi$  plane.

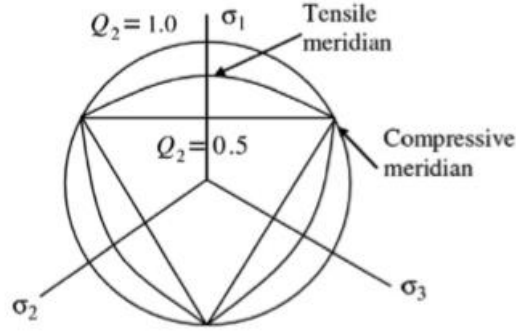


Figure 2.13 Third invariant depend on stress  $\pi$  plane  
Source : ANSYS (2019)

The elastic limit surface is scaled from the failure surface,

$$Y_{elastic} = Y_{fail} \cdot F_{elastic} \cdot F_{cap}(p) \quad 2.4$$

where  $F_{elastic}$  is the ratio of the strength to failure surface strength  $F_{cap}(p)$  is a function that limits the elastic deviatoric stresses under hydrostatic compression, varying within the range of (0,1) for pressure between initial compaction and solid compaction pressure.

The residual failure surface is defined as

$$Y_{residual}^* = B \cdot (p^*)^M \quad 2.5$$

where  $B$  is residual failure surface constant, and  $M$  is residual failure surface exponent.

Following the hardening phase, additional plastic straining of the material results in damage and strength reduction. Damage is assumed to accumulate using the relationship

$$D = \sum \frac{\Delta \epsilon_p}{\epsilon_p^{failure}} = \sum \frac{\Delta \epsilon_p}{D_1 (p^* - p_{spall}^*)^{D_2}} \quad 2.6$$

where  $D_1$  and  $D_2$  are material constants for effective strain to fracture.

The damage accumulation can have two effects in the model, reduction in strength and reduction in shear stiffness as below

$$Y_{fracture}^* = (1 - D)Y_{failure}^* + DY_{residual}^* \quad 2.7$$

$$G_{fracture} = (1 - D)G_{elastic} + DG_{residual} \quad 2.8$$

where  $G_{elastic}$ ,  $G_{residual}$  and  $G_{fracture}$  are the shear modulus.

Magnusson and Hansson (2005) conducted the calibration and validation of the RHT material model on reinforced concrete beam length 1.72 m, subject to blast loading. To simulate the beam response, it was necessary to make some modification of the model. The work concluded that, in the case of blast loading, the principle tensile-failure model was needed to describe the structure behavior rather than the hydrodynamic tensile-failure model used as the default. In the numerical study of reinforced concrete wall subjected to blast loading and fragment loading, Nystrom and Gylltoft (2009) made the same modification to obtain the accurate result.

#### 2.4.2 Material Model for Steel Reinforcement

A Johnson-Cook (JC) material model (Johnson and Cook, 1983) was used to describe the steel reinforcement behaviour. This model represents the strength behaviour of material subject to high strain, high strain rates, and typically metal high temperature. The model defines the yield stress  $Y$  as:

$$Y = [A + B\varepsilon_p^n] \left[ 1 + C \ln \frac{\dot{\varepsilon}_p}{\dot{\varepsilon}_0} \right] [1 - T_H^m] \quad 2.9$$

where  $\varepsilon_p$  is effective plastic strain;  $\dot{\varepsilon}_p = \dot{\varepsilon} / \dot{\varepsilon}_0$  is normalised effective plastic strain rate for  $\dot{\varepsilon}_0 = 1s^{-1}$ ; homologous temperature,  $T_H = (T - T_{room}) / (T_{melt} - T_{room})$  where  $T_{room}$  is room temperature and  $T_{melt}$  is melting temperature; and  $A$ ,  $B$ ,  $C$ ,  $n$  and  $m$  are five material constants. The first, second and third bracket in the equation above represent the stress as a function of strain, effect of strain rate on the yield strength and thermal softening, respectively. The constant  $A$  is the basic yield stress at low strain, while  $B$  and  $n$  represent the effect of strain hardening. Besides the JC material model, Nystrom

and Gylltoft (2009) also used piecewise and thermal effects to conduct numerical studies on RC wall strip subjected blast loads and fragment loading.

### 2.4.3 Material Model for Air and High Explosive

The Arbitrary Lagrange Euler (ALE) is the numerical approach to the air and structure interface analysis. By using this approach, Lagrange and Euler approaches can simultaneously model different parts of the solvers such as structure, fluids and gases. Then, in space and time, these different solvers are coupled.

In the numerical model, air is modelled by an ideal gas EOS, which is one of the simplest forms of EOS. The pressure is related to energy is given by

$$p = (\gamma - 1)\rho e \quad 2.10$$

where  $\gamma$  is a ratio of specific heat and  $\rho$  is air density,  $e$  is the specific internal energy, with the gamma law EOS under standard atmosphere pressure and  $\gamma=1.4$ , its initial energy is  $e=2.068 \times 10^5$  kJ/kg.

TNT the high explosives are typically modelled by using the Jones-Wilkins-Lee (JWL) EOS, which model the pressure generated by chemical energy and can be represented as follows:

$$P = A \left(1 - \frac{\omega}{R_1 V}\right) e^{-R_1 V} + B \left(1 - \frac{\omega}{R_2 V}\right) e^{-R_2 V} + \frac{\omega E}{V} \quad 2.11$$

where  $P$  is the detonation pressure of high explosive;  $V$  is the specific volume;  $E$  is specific internal energy; and  $A$ ,  $B$ ,  $R_1$ ,  $R_2$  and  $\omega$  are material constant which is have been determined form dynamic experiments.

### 2.4.4 Erosion Model

Erosion is a numerical mechanism for the automatic removal of element during simulation. The main reason for using erosion is to remove highly distorted elements from simulation before inverting the elements (ANSYS, 2019). Due to the displacement of the Lagrange grid, Lagrangian material will be subject to major distortions. This leads to the numerical calculation being inaccurate and terminated (Leppänen, 2002). Severely

distorted element in Lagrangian calculation would result in a very small time-step because it is based on the smallest element in the grid and leads to the use of numerous computational cycles (Zukas, 2004). Therefore, erosion ensures that the stability step is maintained at a reasonable level and solutions can continue at the desired termination time.

## **2.5 Summary**

Several studies on the RC wall structures subjected to the blast load based on experimentally and numerically are discussed in this chapter based on the journals, books, internet and research articles. On the numerical studies that related to the blast load, the ANSYS AUTODYN were used to validate to understand the behaviour of the RC structures. This chapter also determine the various of blast load classifications and the characteristics due to the blast load impact. It also study how the blast profile pressure occur. This energy forces the explosive gas to expand and move outward from the detonation centre resulting in a compressed air layer called the blast wave. The sub section of the blast load classification can be divided based on either unconfined or confined explosion containment of the explosive charge. The sub section of RC wall describes the experimental that have been conducted using numerical simulation and the behaviour of the blast overpressure and the behaviour of the RC wall. The sub section of the numerical simulation are focuses on the concept of the AUTODYN software.

## **CHAPTER 3**

### **METHODOLOGY**

#### **3.1 Introduction**

This chapter describes the methodology carried out for the present research that have been made. This research can be divided into four categories. The first part present the blast overpressure based on the literature of Yan et al. (2011). The research is numerical simulation of 13.61 kg (30 lbs.) TNT in the free field. The second part present the numerical simulation of 13.61 kg (30 lbs.) TNT due to the RC solid wall. The third part explain the numerical simulation of the RC solid wall with 25% of circle opening while the fourth part shows the numerical simulation of the blast load due to the RC solid wall with 50% of circle opening. The distance between the 30 lbs TNT explosive from the centre of the weight charge and behind the RC wall at 4ft are considered. When the blast explode, the pressure of the blast will occur and hit behind and surrounding the RC wall. The ANSYS AUTODYN software will be use to simulate the blast wave pressure surrounding the RC wall. The objective of this study are to investigate the blast over the pressure of 30 lbs TNT parameter and to study the effect on blast pressure due to the RC wall with circle opening. The present research can be translated into flowchart as explained in Figure 3.1.



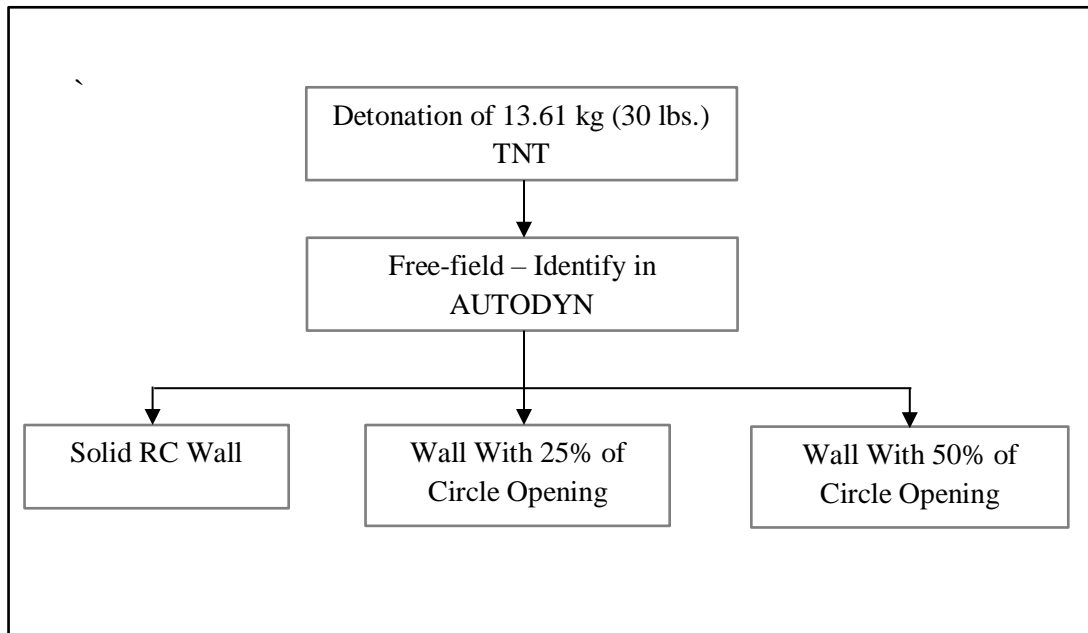


Figure 3.1 The flow chart of research framework

### 3.2 Numerical Modelling RC Wall Subjected to Blast Load in AUTODYN

In this study, AUTODYN is used for numerical analysis. Due to its ability to integrate Lagrangian and Eulerian techniques, AUTODYN is selected which allows for the possible assessment of blast overpressure and its impact on the structure in this study. The ALE (Arbitrary Lagrange Euler) solve is used as it is a mesh-based hybrid between the Lagrangian and Eulerian method as shown in Figure 3.2.

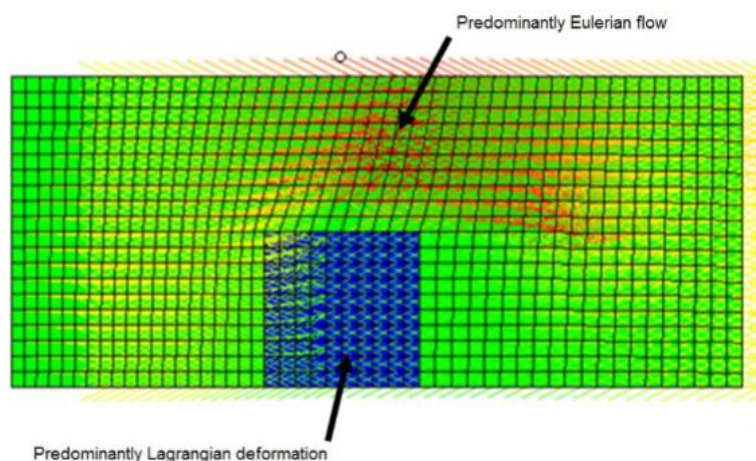


Figure 3.2 ALE solver technique in AUTODYN  
Source : ANSYS (2019)

The identification of the solid elements used is performed in ANSYS-Workbench before the RC wall can be exported to AUTODYN solver for blast and impact analysis. The line body is used and treated as an ideal bond between steel reinforcement and concrete in the evaluation for the metal reinforcement in the concrete. Figure 3.3 shows the eight nodes hexahedral element used for solid element. This element is well suited to the transient dynamic applications including large deformations, large strains, large rotations and complex contact conditions. Based on the research of Wilkins et al. (1974), the element formulation results in a precise calculation of the quantity even for distorted elements.

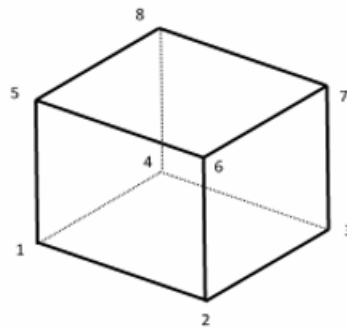


Figure 3.3 Eight nodes hexahedral element  
Source : ANSYS (2019)

Figure 3.4 illustrate the detail of the RC wall employed in thus study. The reinforced with 16 mm diameter at 152 mm spacing. The concrete that covers all sides of the wall is 25 mm thick. The cylinder compressive strength of the concrete is 44 MPa with a standard deviation of 1.38 MPa while the Modulus of Elasticity is 31.5 GPa with a standard deviation of 827 MPa. The reinforcement has a yield strength of 619 MPa and a Young's modulus of 200 GPa. The walls have a cross-sectional dimension of 1829 mm x 1219 mm with the wall thickness of 150 mm and 305 mm thickness of footing. The circle opening on the RC wall has a dimension with 50 mm radius. Figure 3.5 illustrate the solid RC wall replaced with solid RC wall with 25% of circle opening (a) and with solid RC wall with 50% of circle opening (b). Figure 3.6 shows the RC wall meshed with the coarse hexahedral element.

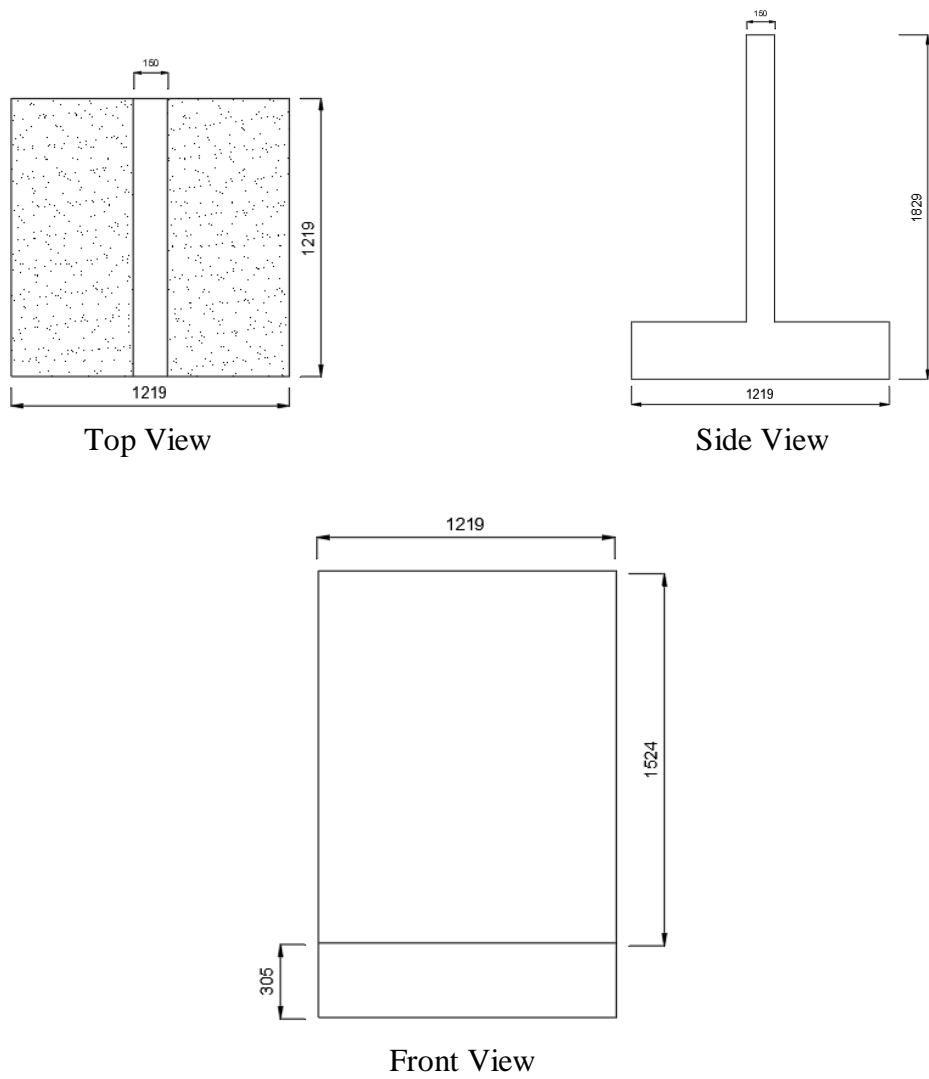


Figure 3.4 Detail of solid RC wall

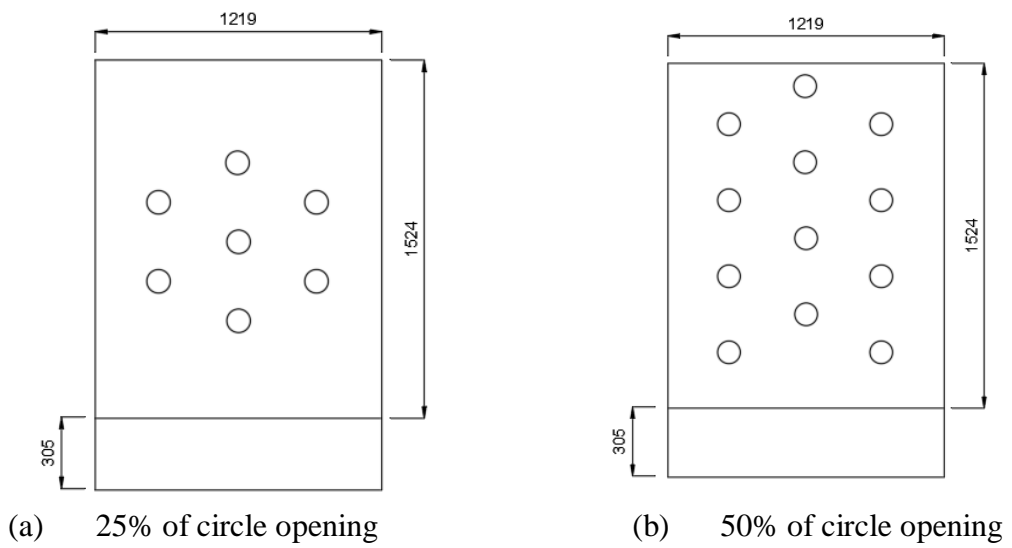


Figure 3.5 Detail of RC wall with circle opening

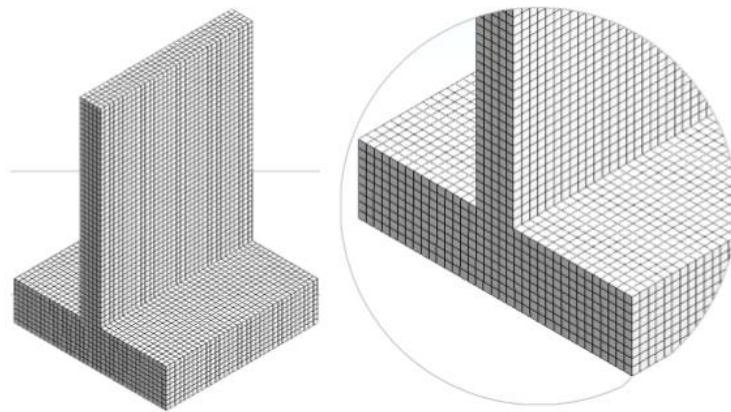


Figure 3.6 Hexahedral meshing of RC wall

The standard material model for 35 MPa (CONC-35MPA) concrete in the material library of the AUTODYN is used to describe the concrete behaviour. Riedel, Hiermayer and Thoma (RHT) developed this material model (Riedel et al., 1999). Thus, the standard STEEL-4340 model in the AUTODYN material library is used to describe the behaviour of steel reinforcement. Johnson and Cook (JC) (Johnson and Cook, 1983) developed this material model and is known as the JC model. Both materials are presented in Table 3.1 and Table 3.2 respectively. The concrete compressive strength and steel yield stress are changed accordingly for the preliminary numerical studies based on the RC wall built by Yan et al. (2011).

Table 3.1 Employed material data for concrete, input data to the RHT model

<b>Equation of state</b>	<b>P alpha</b>
Reference density	2.75000E+00 (g/cm <sup>3</sup> )
Porous density	2.31400E+00 (g/cm <sup>3</sup> )
Porous soundspeed	2.92000E+03 (m/s)
Initial compaction pressure	2.33000E+04 (kPa)
Solid compaction pressure	6.00000E+06 (kPa)
Compaction exponent	3.00000E+00 (none)
Solid EOS	Polynomial
Bulk Modulus A1	3.52700E+07 (kPa)
Parameter A2	3.95800E+07 (kPa)
Parameter A3	9.04000E+06 (kPa)
Parameter B0	1.22000E+00 (none)
Parameter B1	1.22000E+00 (none)
Parameter T1	3.52700E+07 (kPa)
Parameter T2	0.00000E+00 (kPa)
Reference temperature	3.00000E+02 (K)
Specific heat	6.54000E+02 (J/kgK)
Thermal conductivity	0.00000E+00 (J/mKs)
Compaction curve	Standard
<b>Strength</b>	<b>RHT Concrete</b>
Shear modulus	1.67000E+07 (kPa)
Compressive strength (fc)	3.50000E+04 (kPa)
Tensile strength (ft/fc)	1.00000E-01 (none)
Shear strength (fs/fc)	1.80000E-01 (none)
Intact Failure Surface Constant A	1.60000E+00 (none)
Intact Failure Surface Exponent N	6.10000E-01 (none)
Tens./Comp. Meridian Ratio (Q)	6.80500E-01 (none)
Brittle to Ductile Transition	1.05000E-02 (none)
G (elas.)/(elas.-plas.)	2.00000E+00 (none)
Elastic Strength / ft	7.00000E-01 (none)
Elastic Strength / fc	5.30000E-01 (none)
Fractured Strength Constant B	1.60000E+00 (none)
Fractured Strength Exponent M	6.10000E-01 (none)
Compressive Strain Rate Exp. Alpha	3.20000E-02 (none)
Tensile Strain Rate Exp. Delta	3.60000E-02 (none)
Max. Fracture Strength Ratio	1.00000E+20 (none)
Use CAP on Elastic Surface?	Yes
<b>Failure</b>	<b>RHT Concrete</b>
Damage Constant, D1	4.00000E-02 (none)
Damage Constant, D2	1.00000E+00 (none)
Minimum Strain to Failure	1.00000E-02 (none)
Residual Shear Modulus Fraction	1.30000E-01 (none)
Tensile Failure	Hydro (Pmin)
<b>Erosion</b>	<b>Geometric Strain</b>
Erosion Strain	2.00000E+00 (none)
Type of Geometric Strain	Instantaneous

Source : ANSYS (2019)

Table 3.2 Employed material data for steel reinforcement, input data to the JC model

<b>Equation of state</b>	<b>Linear</b>
Reference density	7.83000E+00 (g/cm <sup>3</sup> )
Bulk modulus	1.59000E+08 (kPa)
Reference temperature	3.00000E+02 (K)
Specific heat	4.77000E+02 (J/kgK)
Thermal conductivity	0.00000E+00 (J/mKs)
<b>Strength</b>	<b>RHT Concrete</b>
Shear modulus	7.70000E+07 (kPa)
Yield Stress	7.92000E+05 (kPa)
Hardening constant	5.10000E+05 (kPa)
Hardening exponent	2.60000E-01 (none)
Strain rate constant	1.40000E-02 (none)
Thermal softening exponent	1.03000E+00 (none)
Melting temperature	1.79300E+03 (K)
Ref. Strain Rate (/s)	1.00000E+00 (none)
Strain rate correction	1st Order
<b>Failure</b>	<b>RHT Concrete</b>
Damage Constant, D1	5.00000E-02 (none)
Damage Constant, D2	3.44000E+00 (none)
Damage Constant, D3	-2.12000E+00 (none)
Damage Constant, D4	2.00000E-03 (none)
Damage Constant, D5	6.10000E-01 (none)
Melting Temperature	1.79300E+03 (K)
Ref. Strain Rate (/s)	1.00000E+00 (none)
<b>Erosion</b>	<b>None</b>

Source : ANSYS (2019)

In the AUTODYN, the initial explosive and blast wave propagation detonation is modelled with a wedge-shaped axial symmetry. The wedge filled with the calculated load circle for TNT material model 13.61 kg (30 lbs.) and the remaining area outside the circle is filled with the model of air material as shown in Figure 3.7. As shown in Figure 3.8, the detonation is initiated and run until the blast wave reached 1 m from the centre of detonation. The "fill" file consists of the history of blast overpressure being created and will be used in other types of 3D air volume for further remapping function.

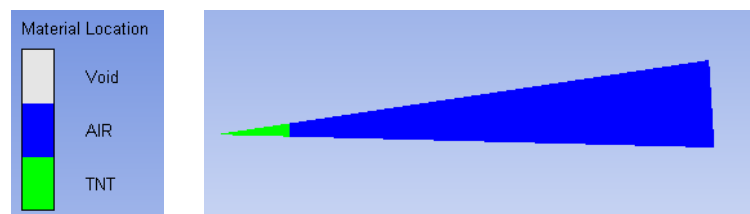


Figure 3.7 The 1m wedge (2D) filled with TNT and air

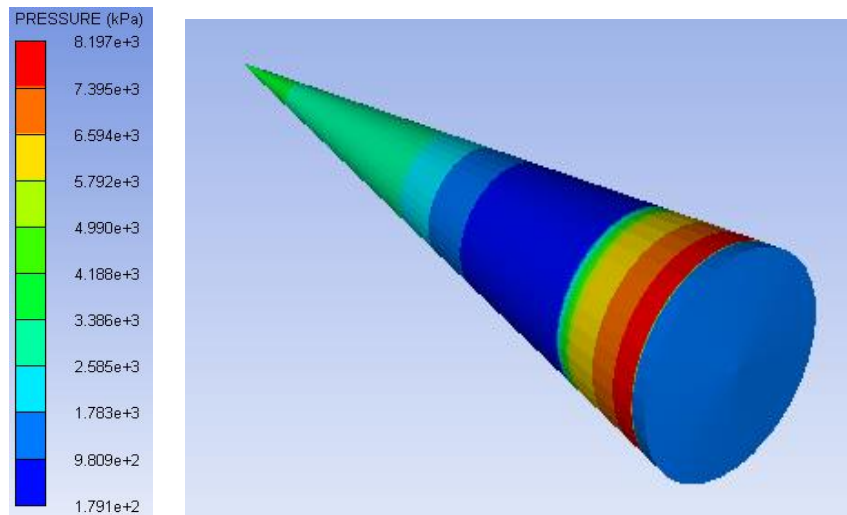


Figure 3.8 Pressure contours in 1m wedge (3D) during solving progress

The standard air constant in the material library of the AUTODYN is used to describe the air behaviour being modelled through the ideal state gas expression (EOS). Then, to describe the behaviour of the explosive, Jones-Wilkins-Lee EOS ' standard TNT model is used where Dobratz and Crawford (1985) parameters are implemented. Both material properties are listed in Table 3.3 and Table 3.4, respectively.

Table 3.3 Employed material data for air, input data to the ideal gas EOS

<b>Equation of state</b>	<b>Ideal Gas</b>
Reference density	1.22500E-03 (g/cm <sup>3</sup> )
Gamma	1.40000E+00 (none )
Adiabatic constant	0.00000E+00 (none )
Pressure shift	0.00000E+00 (kPa )
Reference temperature	2.88200E+02 (K )
Specific heat	7.17600E+02 (J/kgK )
Thermal conductivity	0.00000E+00 (J/mKs )
<b>Strength</b>	<b>None</b>
<b>Failure</b>	<b>None</b>
<b>Erosion</b>	<b>None</b>

Source : ANSYS (2019)

Table 3.4 Employed material data for TNT, input data to the JWL EOS

<b>Equation of state</b>	<b>JWL</b>
Reference density	1.63000E+00 (g/cm <sup>3</sup> )
Parameter A	3.73770E+08 (kPa)
Parameter B	3.74710E+06 (kPa)
Parameter R1	4.15000E+00 (none)
Parameter R2	9.00000E-01 (none)
Parameter W	3.50000E-01 (none)
C-J Detonation velocity	6.93000E+03 (m/s)
C-J Energy / unit volume	6.00000E+06 (kJ/m <sup>3</sup> )
C-J Pressure	2.10000E+07 (kPa)
Burn on compression fraction	0.00000E+00 (none)
Pre-burn bulk modulus	0.00000E+00 (kPa)
Adiabatic constant	0.00000E+00 (none)
Auto-convert to Ideal Gas	Yes
Additional Options (Beta)	None
<b>Strength</b>	<b>None</b>
<b>Failure</b>	<b>None</b>
<b>Erosion</b>	<b>None</b>

Source : ANSYS (2019)

### 3.2.1 Blast Overpressure Analysis

Initially, the air volume Type 1 is used to assess the blast overpressure of the calculated explosive (TNT charge circle) in a free field explosion without taking into consideration of the RC wall structure as suggested by Luccioni et al. (2006). The other three air volume types considered the RC wall such as air volume Type 2, Type 3 and Type 4. Type 3 considered the RC wall with 25% of circle opening while Type 4 considered the RC wall with 50% of circle opening.

#### 3.2.1.1 Air Volume Type 1

Figure 3.9 shows the 3D model and the remapped blast overpressure vectors in air volume Type 1. Pressure Gauge are placed at 5486 mm (18 ft.) away from the centre of the charge weight. The air domain are created and the outflow boundary will be insert surrounding the air domain.



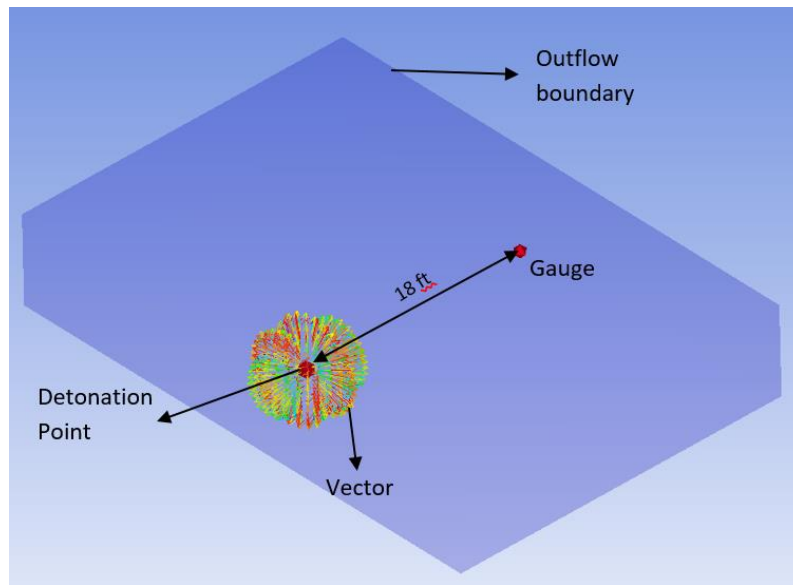


Figure 3.9 Blast simulation in free-field

### 3.2.1.2 Air Volume Type 2

Figure 3.10 shows the 3D model and the remapped blast overpressure vectors in air volume Type 2 with the consideration of solid RC wall. Five pressure gauges are placed from the centre of the charge weight. Gauge 1 and Gauge 2 are placed at 1219 mm (4 ft.) and 2438 mm (8 ft.), respectively. While Gauge 3 and Gauge 4 are placed at 3657 mm (12 ft.) and 4876 mm (16 ft.) away from the charge of the weight. Gauge 5 is positioned which is 5486 mm (18 ft.) from the centre of the wall.

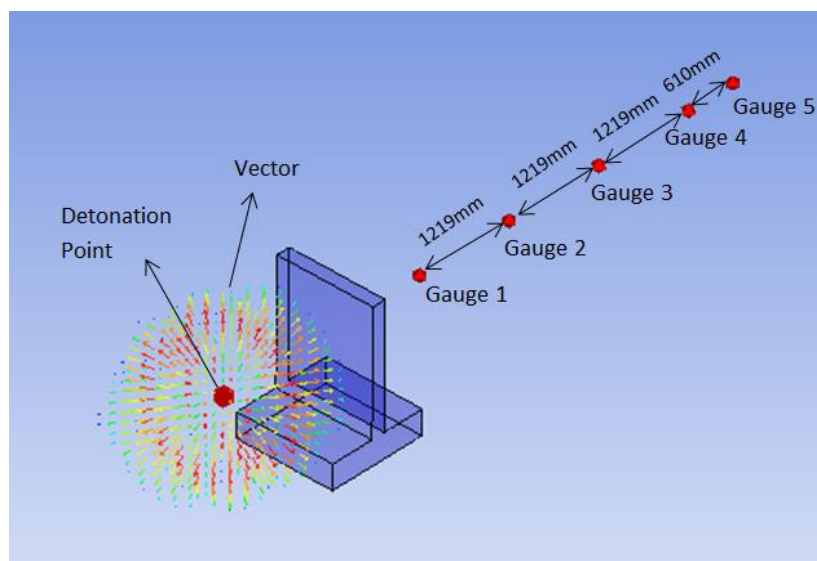


Figure 3.10 Blast simulation on solid RC wall

### 3.2.1.3 Air Volume Type 3

Figure 3.11 illustrates the 3D model and the remapped blast overpressure vectors in air volume Type 3 with consideration of RC wall with 25% of circle opening. The same distance and location of the pressure gauges from the explosive in the air volume Type 2 are assigned for the RC wall on Type 3.

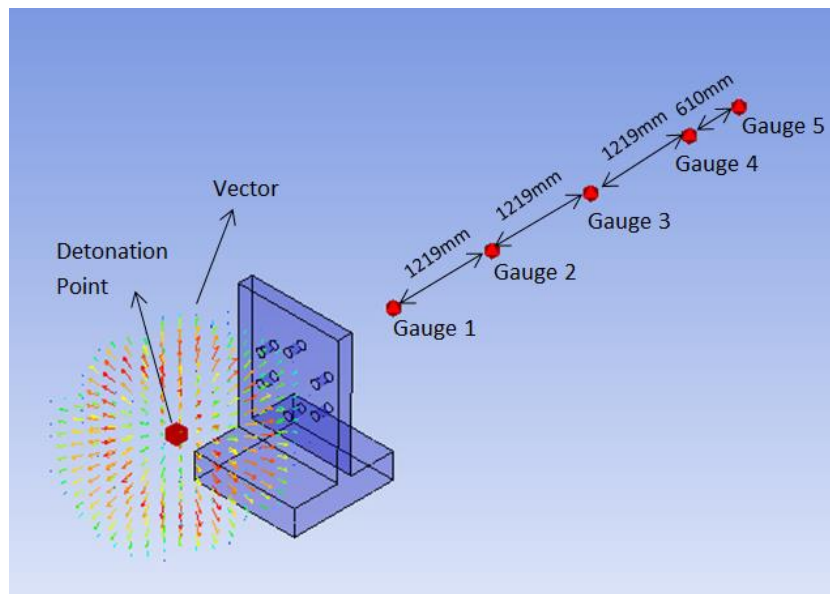


Figure 3.11 Blast simulation on solid RC wall with 25% of circle opening

### 3.2.1.4 Air Volume Type 4

Figure 3.12 illustrates the 3D model and the remapped blast overpressure vectors in air volume Type 4 with the consideration of RC wall with 50% of circle opening. The same distance and location of the pressure gauges from the explosive in the air volume Type 2 and Type 3 are assigned for the RC wall on Type 3.

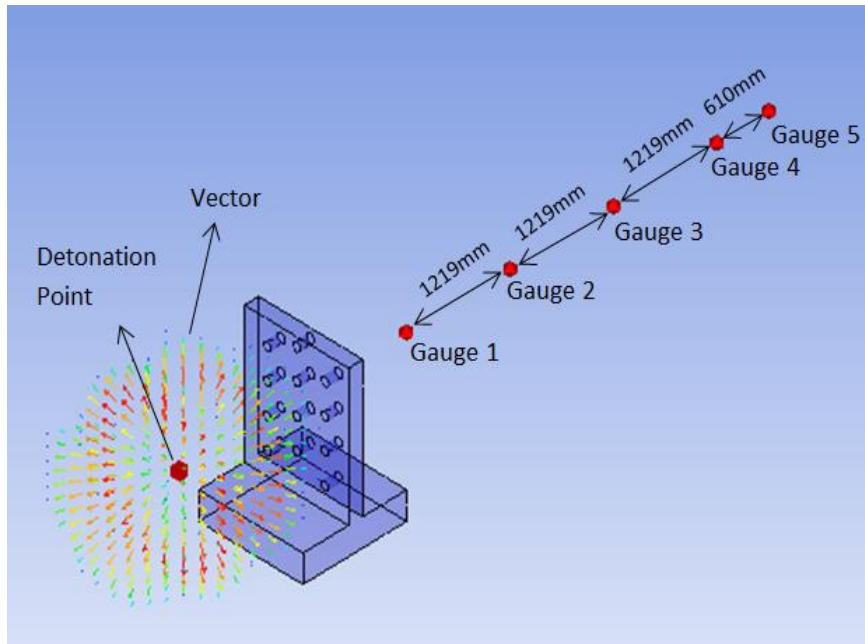


Figure 3.12 Blast simulation on solid RC wall with 50% of circle opening

### 3.3 Summary

This chapter shows the methodology carried out for the present research. This research can be divided into four parts, free-field based on research by Yan et al. (2011), solid RC wall, solid RC wall with 25% of circle opening and solid RC wall with 50% of circle opening. The location of the pressure gauge are similarly to the Type 2, Type 3 and Type 4, such as, 1219 mm (4 ft.), 2438 mm (8 ft.), 3657 mm (12 ft.), 4876 mm (16 ft.) and 5486 mm (18 ft.). There are three types of the detail of the RC wall that use in this study. There are solid RC wall, solid RC wall with 25% of circle opening and solid RC wall with 50% of circle opening. There are also several employed material data for this research that have been used, such as, concrete, steel reinforcement, air and TNT. The material data for all the material that used in this research are defined in the source of the ANSYS AUTODYN (2019). The wedge filled with the calculated load circle for TNT material model 13.61 kg (30 lbs.) and the remaining area outside the circle is filled with the model of air material. The detonation is initiated and run until the blast wave reached 1 m from the centre of detonation. The "fill" file consists of the history of blast overpressure being created and will be used in other types of 3D air volume for further remapping function.

## **CHAPTER 4**

### **RESULTS AND DISCUSSION**

#### **4.1 Introduction**

This chapter presents the analysis of blast overpressure parameter and its impact on the RC solid wall and RC solid wall with circle opening. This analysis divided into four part sections. The first part present the blast overpressure analysis of 13.61 kg (30 lbs.) TNT charge weight at located 5486 mm (18 ft.) away on the free-field space. This research compared the blast overpressure parameters as reported by Yan et al. (2011) of the blast overpressure parameters. The second part present the blast overpressure analysis of 13.61 kg (30 lbs.) TNT charge weight located at 1219 mm (4 ft.) away from the RC solid wall. The third part shows the blast overpressure analysis of 13.61 kg (30 lbs.) TNT charge weight at located at 1219 mm (4 ft.) away from the RC wall with 25% of circle opening while fourth part also similar to the third part but replaced with RC solid wall with 50% of circle opening.

#### **4.2 Blast Overpressure Analysis in AUTODYN**

The following sub-chapter explain the numerically simulated blast overpressure of 13.61 kg (30 lbs.) TNT charge weight in different air volume type.

##### **4.2.1 Air Volume Type 1**

Figure 4.1 shows the comparison of the simulated blast overpressure at 5486 mm (18 ft.) away with peak blast overpressure of 494.46 kPa at 4.62 msec and the blast overpressure recorded in the blast test reported by Yan et al. (2011). The simulated peak overpressure is close to the recorded blast overpressure in blast test by Yan et al. (2011) with 490 kPa at 4.64 msec, but the blast overpressure duration falls back to the ambient pressure and was found to be longer than the 14.7 msec and 6.6 msec blast test

respectively. This behaviour is similar to the numerical modeling research works carried out by Sivakumar et al. (2011) and Kim et al. (2009) in which the simulated impact of blast overpressure was successfully validated by the actual impact of the blast. The defined TNT charge weight of 13.61 kg (30 lbs.) is valid and can replicate the actual blast overpressure in the current numerical 3D modelling.

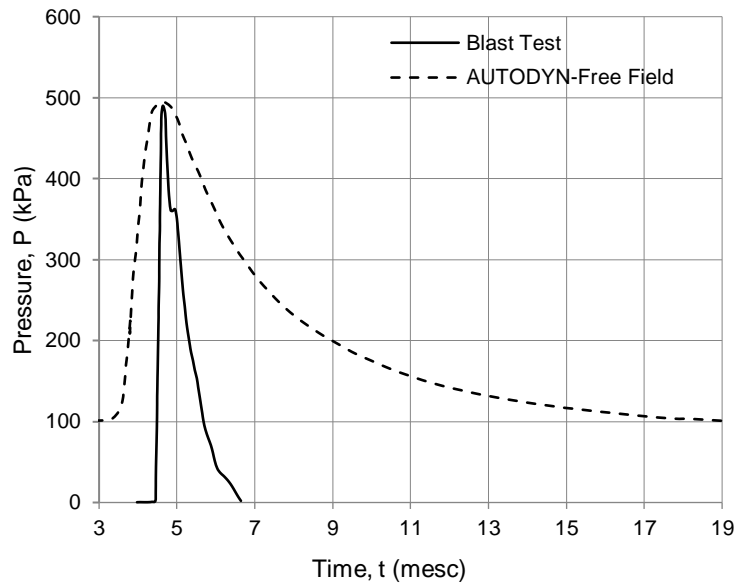


Figure 4.1 Comparison blast overpressure-time history

#### 4.2.2 Air Volume Type 2

Figure 4.2 shows the result of the blast overpressure with the consideration of solid RC wall. The pressure gauge are placed at five different distance and location, Gauge 1 and Gauge 2 are placed at 1219mm (4 ft.) and 2438 mm (8 ft.), respectively. While Gauge 3 and Gauge 4 are placed at 3657 mm (12 ft.) and 4876 mm (16 ft.), respectively. Then, Gauge 5 is placed on at 5486 mm (18 ft.) away from the charge of the weight. It is found that the highest peak blast overpressure on the Gauge 1 at 1219 mm distance with 0.29 MPa at 1.25 msec, followed by Gauge 2 at 1829 mm and Gauge 3 at 3048 mm with 0.19 MPa at 2.89 msec and 0.16 MPa at 5.22 msec, respectively. For the blast pressure Gauge 4 at 4267 mm is 0.14 MPa at 7.65 msec, while Gauge 5 is 0.14 MPa at 8.82 msec at 5486 mm distance from the charge weight.

Figure 4.3 illustrates the blast wave vectors propagation of solid RC wall until reached pressure gauge at 5486 mm (18 ft.) away. It shows that the starting of the blast

vector until the blast vector reached until 5486 mm (18 ft.) away from the centre of charge weight. The blast vector start from 0 msec of the process of blast propagation at 1219 mm (4 ft.) from the charge weight. Then the blast vector will start expand and hit the surface of the RC wall. It will go further surrounding the RC wall until it reached the accurate result.

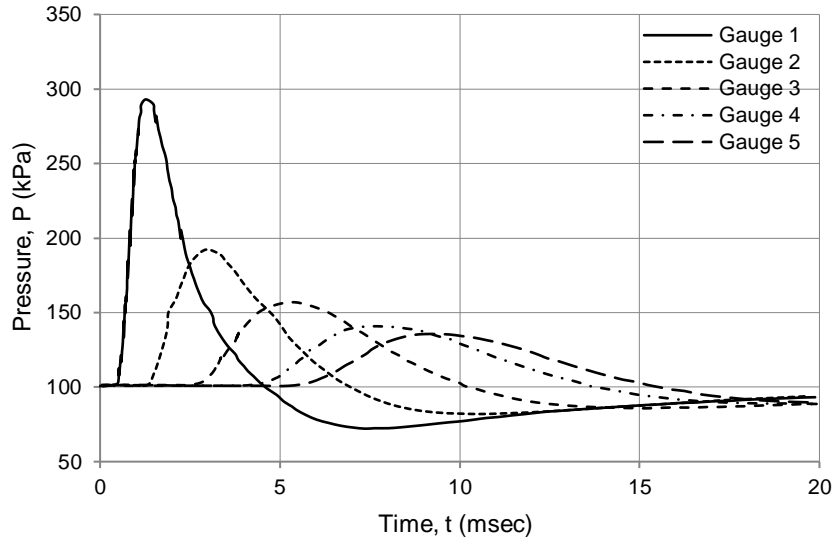


Figure 4.2 Blast overpressure-time history in Type 2

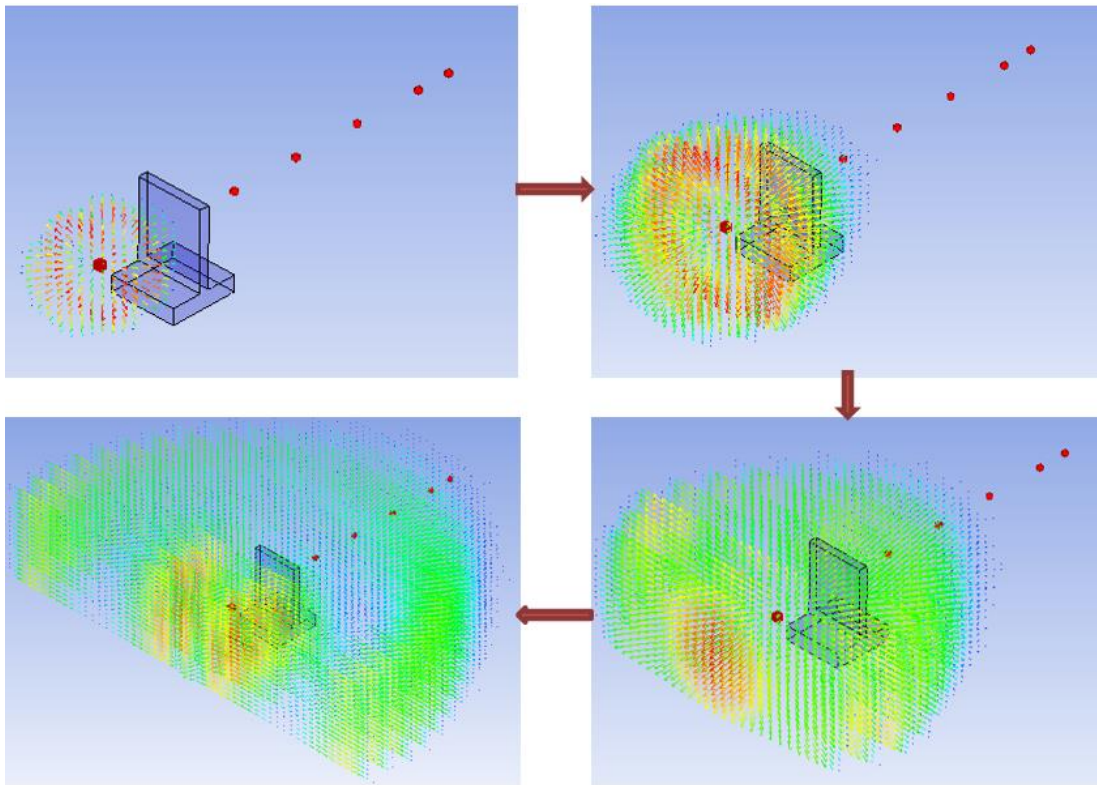


Figure 4.3 Blast vectors propagation of solid RC wall

### 4.2.3 Air Volume Type 3

According to Figure 4.4, it shows that the blast overpressure with the consideration of RC wall with 25% circle of opening. The arrangement of the pressure gauge same with Type 2. The pressure gauge are placed at five different distance and location, Gauge 1 and Gauge 2 are placed at 1219mm (4 ft.) and 2438 mm (8 ft.), respectively. While Gauge 3 and Gauge 4 are placed at 3657 mm ( 12 ft.) and 4876 mm (16 ft.), respectively. Then, Gauge 5 is placed on at 5486 mm (18 ft.) away from the charge of the weight. According to Figure 4.5, it is found that the highest peak blast pressure is on the Gauge 1 that from 1219 mm from the charge weight with 0.29 MPa at 1.06 msec, followed by Gauge 2 and Gauge 3 with 0.19 MPa at 2.73 msec and 0.16 MPa at 5.02 msec, respectively. Then, the peak blast pressure for Gauge 4 at 4267 mm is 0.14 MPa at 7.59 msec, while for Gauge 5 is 0.14 MPa at 8.79 msec at 5486 mm distance from the centre of the wall.

Figure 4.5 illustrates the blast wave vectors propagation of solid RC wall with 25% circle opening until reached pressure gauge at 5486 mm (18 ft.) away. It shows that the starting of the blast vector until the blast vector reached until 5486 mm (18 ft.) away from the centre of charge weight. The blast vector start from 0 msec of the process of blast propagation at 1219 mm (4 ft.) from the charge weight. Then the blast vector will start expand and hit the surface of the RC wall. It will go further surrounding the RC wall until it reached the accurate result.

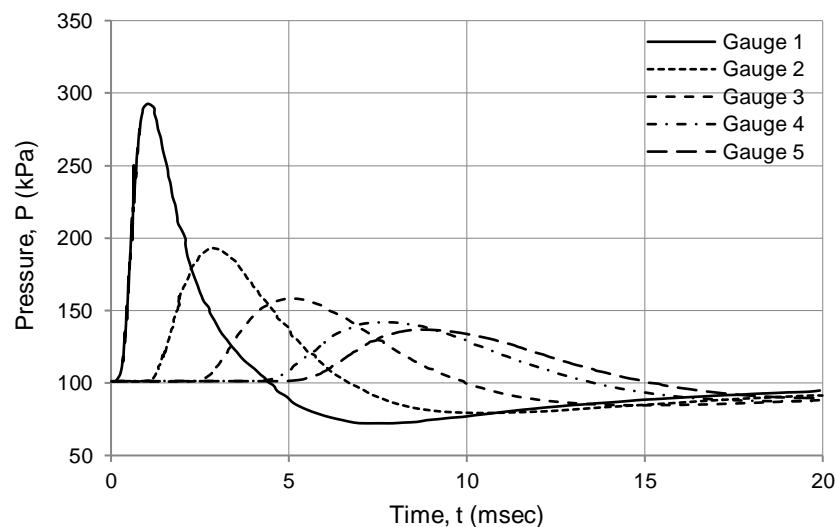


Figure 4.4 Blast overpressure-time history in Type 3

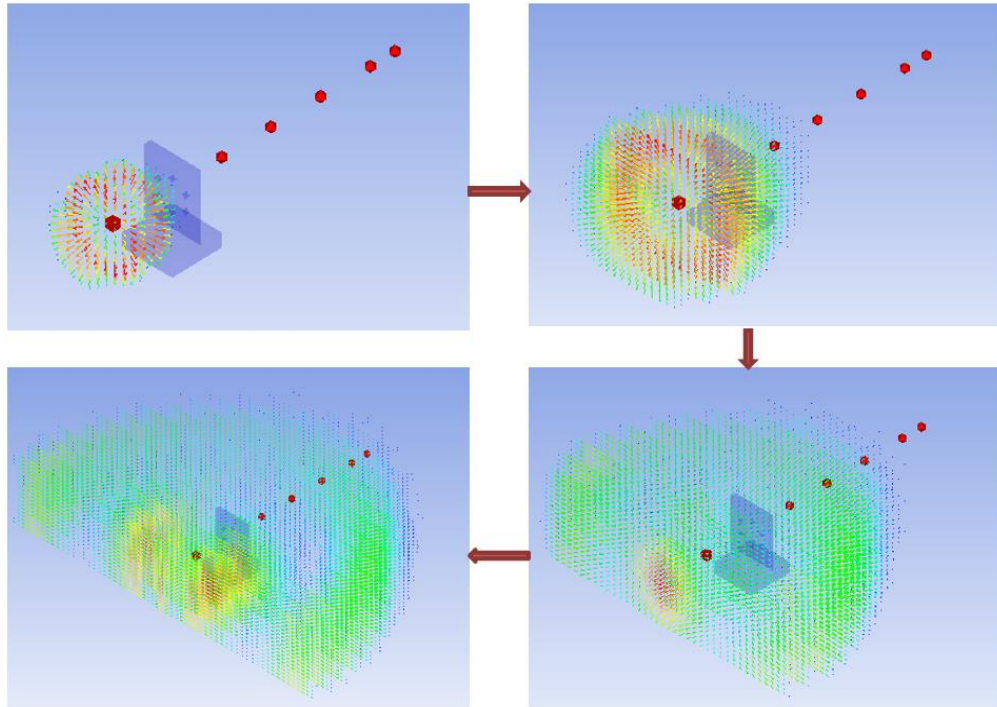


Figure 4.5 Blast vectors propagation of solid RC wall with 25% of circle opening

#### 4.2.4 Air Volume Type 4

Based on Figure 4.6, the result of blast overpressure with the consideration of RC wall with 50% of circle opening. The location and the distance of the pressure gauge same as the Type 2 and Type 3. The pressure gauge are placed at five different distance and location, Gauge 1 and Gauge 2 are placed at 1219mm (4 ft.) and 2438 mm (8 ft.), respectively. While Gauge 3 and Gauge 4 are placed at 3657 mm ( 12 ft.) and 4876 mm (16 ft.), respectively. Then, Gauge 5 is placed on at 5486 mm (18 ft.) away from the charge of the weight. The result found that Gauge 1 is the highest blast pressure that is 0.29 MPa at 1.04 msec from 1219 mm from the centre of charge weight. Gauge 2 is the second highest blast pressure with 0.19 MPa at 2.77 msec, followed by Gauge 3 that found the pressure is 0.16 MPa at 5.01 msec. Then, Gauge 4 at 4267 mm with 0.14 MPa at 7.62 msec, while Gauge 5 with 0.14 MPa at 8.76 msec.

Figure 4.7 illustrates the blast wave vectors propagation of solid RC wall with 50% circle opening until reached pressure gauge at 5486 mm (18 ft.) away. It shows that the starting of the blast vector until the blast vector reached until 5486 mm (18 ft.) away from the centre of charge weight. The blast vector start from 0 msec of the process of



blast propagation at 1219 mm (4 ft.) from the charge weight. Then the blast vector will start expand and hit the surface of the RC wall. It will go further surrounding the RC wall until it reached the accurate result.

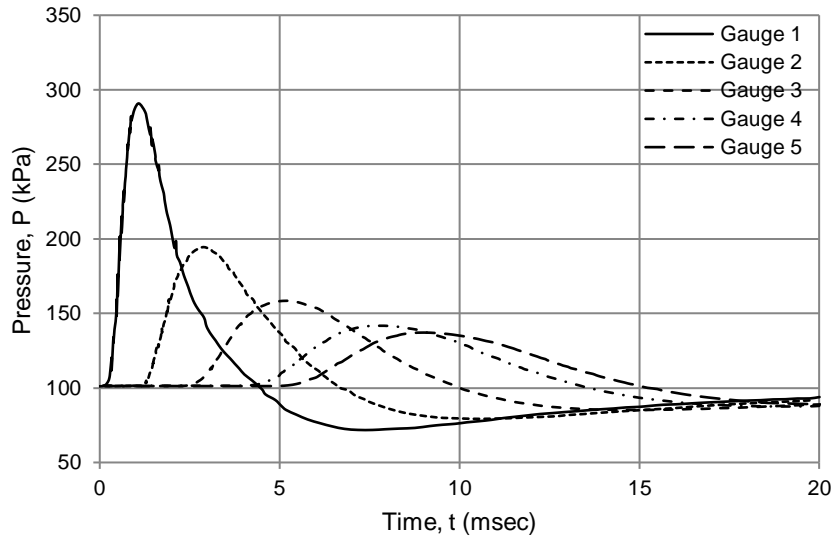


Figure 4.6 Blast overpressure-time history in Type 4

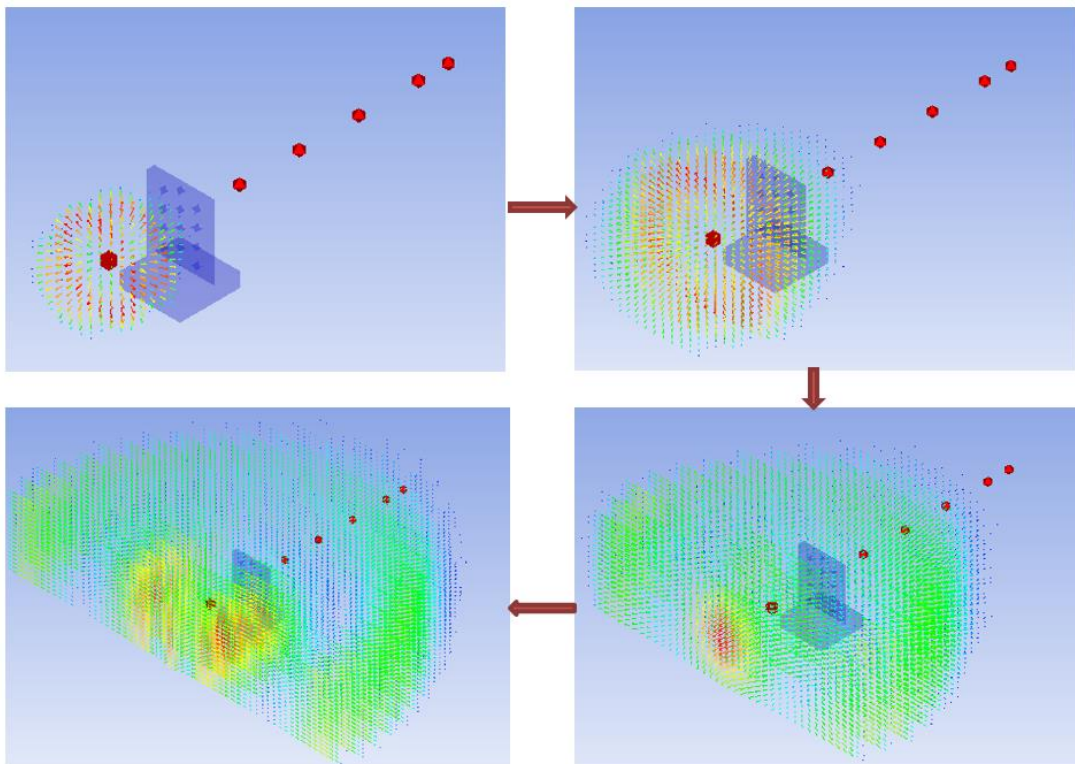


Figure 4.7 Blast vectors propagation of solid RC wall with 50% of circle opening

### 4.3 Comparison of Peak Blast Overpressure between All Type of Air Volume

#### 4.3.1 Type 2 with Type 3 of Blast Overpressure

From the recorded peak blast overpressure in Table 4.1, the average of the overall pressure gauge has percentage difference between 0.19% until 1.19% in range. So, the blast pressure between solid RC wall (Type 2) with wall with 25% circle of opening (Type 3) are similarly to each other in the term of the blast pressure parameters. It is because of the type of RC wall have same criteria and properties but different in the term of shape of opening of the RC wall. The blast overpressure parameters approximately similar compared with solid RC wall and wall with 50% of circle opening. It is possible to use RC wall with circle opening to replace solid RC wall because wall with circle opening give more aesthetic value and good view in the term of architectural.

Table 4.1 Comparison of peak blast overpressure-time history between Type 2 and Type 3

Gauge No.	Pressure of Type 2 (kPa)	Pressure of Type 3 (kPa)	Percentage Difference (%)
1	293.3	293.7	0.14
2	191.6	193.9	1.19
3	157.1	158.3	0.76
4	141.2	141.8	0.42
5	136.0	136.8	0.59

#### 4.3.2 Type 2 with Type 4 of Blast Overpressure

From the recorded peak blast overpressure in Table 4.2, the average of the overall pressure gauge has percentage difference between 0.07% until 1.50% in range. So, the blast pressure between solid RC wall (Type 2) with wall with 50% circle of opening (Type 4) are similarly to each other in the term of the blast pressure parameters. It is because of the type of RC wall have same criteria and properties but different in the term of shape of opening of the RC wall. The blast overpressure parameters approximately similar compared with solid RC wall and wall with 25% of circle opening. It is possible to use RC wall with circle opening to replace solid RC wall because wall with circle opening give more aesthetic value and good view in the term of architectural. The volume of the concrete will be reduced due to the shape of opening of the RC wall. Thus, it will also save the cost of the structure but still valid as the protection wall barrier.

Table 4.2 Comparison of peak blast overpressure-time history between Type 2 and Type 4

Gauge No.	Pressure of Type 2 (kPa)	Pressure of Type 4 (kPa)	Percentage Difference (%)
1	293.3	293.5	0.07
2	191.6	194.5	1.50
3	157.1	158.4	0.82
4	141.2	142.0	0.56
5	136.0	137.0	0.73

#### 4.4 Summary

By conducting analysis and discussion in this chapter, RC solid wall and RC solid wall with circle opening give the approximately similar in the term of blast overpressure parameters. So, it is possible to replace the solid RC wall with solid RC wall with circle opening because the wall give more aesthetic value and economical product. When the wall with circle opening used in the civilian, it give good view in to view different types of RC wall that have circle opening. If the RC wall with circle opening used in the construction, it reduce the volume of the concrete usage then it reduce cost too but it still valid to use as protection. From the recorded blast overpressure, it shown that the result between the all Type, it has between 0.07% until 1.50% percentage difference between RC solid wall, wall with 25% circle opening, wall with 50% circle opening.

## CHAPTER 5

### CONCLUSIONS AND RECOMMENDATIONS

#### 5.1 Conclusions

The following are conclusions arrived through the numerical simulation investigation of RC solid wall and RC solid wall with circle opening subjected to 13.61 kg (30 lbs.) TNT blast overpressure:

1. Numerical simulation has been performed to simulate the blast propagation and overpressure study on the RC solid wall, RC solid wall with 25% of circle opening and RC solid wall with 50% of circle opening.
2. The numerical result shows that blast overpressure between the RC solid wall (Type 2), RC solid wall with 25% of circle opening (Type 3) and RC solid wall with 50% of circle opening (Type 4) are similarly in the term of blast pressure parameters.
3. The pressure gauge that close to the charge weight of blast, such as 1219 mm (4ft), it will give higher value of blast overpressure. Thus, the pressure gauge that far from the detonation charge weight, such as 5486 mm (18ft), the value of blast pressure will be lower due to the distance and impact of the blast load.
4. From the recorded blast overpressure, it shown that the result between the all Type, it has between 0.07% until 1.50% percentage difference between RC solid wall, wall with 25% circle opening, wall with 50% circle opening.

5. The solid RC wall and wall with circle opening made the result approximately similar in the term of blast pressure parameters. It is because of the type of the RC wall have similar criteria and properties of the designation.
6. In conclusion, the RC wall is possible to replace with RC wall with circle opening because the blast pressure are similar compared to the two different shape of opening. When the RC wall with circle opening are used, the volume of the concrete will be reduced. Then, if the volume of concrete decreased, it will saving the cost of the structure and it will reduce the time of the construction. Thus, RC wall with circle opening is valid to use as wall barrier an as aesthetic value.

## **5.2 Recommendations**

Further to the research that has been conducted, there are several actions or further work to be done. The following are some recommendations that should be consider in achieved a better research result:

1. Focusing on the method to use the RC wall with circle opening that will give more effective and economical.
2. RC wall able to use another shape of opening for aesthetic value. For the next few years, RC wall in the construction be able to use another type of opening such as rectangle, square, triangle and others. This will give another better result that if it can reducing in the term of the blast pressure parameters.
3. Possible to use another better percentage of opening that can be used for RC wall. For this study, it use 25% and 50% of circle opening. Thus, it possible to suggest with 30% or 60% to get the better result and will give more in the term of aesthetic value.
4. Decreasing the percentage volume of concrete to save the cost of the structure.

## REFERENCES

- Abdel-Mooty, M., Alhayawei, S. and Issa, M. (2016) 'Performance of one-way reinforced concrete walls subjected to blast loads', *International Journal of Safety and Security Engineering*, 6(2), pp. 406–417. doi: 10.2495/SAFE-V6-N2-406-417.
- Ackland, K., Bornstein, H. and Lamos, D. (2012). An analysis of TNT equivalencies using AUTODYN. *Proceedings of the Australasian Structural Engineering Conference*, pp. 804-811.
- Ali, N. M., Syed Mohsin, S. M., Seman, M.A., Mohd Jaini, Z. (2015) 'Numerical Prediction of Cantilevered Reinforced Concrete Wall Subjected to Blast Load', pp. 1–2. doi: 10.1021/es4049626.
- Alsubaei, F. C. F. (2015) 'Performance of Protective Perimeter Walls Subjected to Explosions in Reducing the Blast Resultants on Buildings', (August).
- ANSYS. (2019). *Release 19.0 R1*. Canonsburg, PA: ANSYS, Inc.
- Appuhamilage, G. (2015) 'Effects of Blast Loading on Reinforced Concrete Facade Systems'. Available at: <http://vuir.vu.edu.au/29785/>.
- Bangash, M.Y.H. (2008). *Shock, Impact And Explosion : Structural Analysis And Design*. London: Springer.
- Braimah, A. and Siba, F. (2017) 'Near-field explosion effects on reinforced concrete columns: an experimental investigation', *Canadian Journal of Civil Engineering*, 45(4), pp. 289–303. doi: 10.1139/cjce-2016-0390.
- Draganic, H. and Sigmund, V. (2012) 'Blast Loading on Structures', *Physical Review A*, 93(3), p. 10. doi: 10.1103/PhysRevA.93.033817.
- Fan, J. (2014) 'Response of Reinforced Concrete Reservoir Walls Subjected to Blast Loading by Master of Applied Science', (April).
- Gaikwad, S. T. and Shirsath, M. N. (2017) 'Study of Blast Analysis for Structural Building', *International Research Journal of Engineering and Technology*, 4(7), pp. 93–95.
- Imperial College London (2004) 'Health & Safety Executive: Analysis and Design of Profiled Blast Walls'.
- Kang, K. Y., Choi, K. H., Choi, J. W., Ryu, Y. H., Lee, J. M. (2017) 'Explosion induced dynamic responses of blast wall on FPSO topside: Blast loading application methods', *International*

*Journal of Naval Architecture and Ocean Engineering*. Elsevier Ltd, 9(2), pp. 135–148. doi: 10.1016/j.ijnaoe.2016.08.007.

MSHA. (1977). Special hazards of acetylene (online). Retrieved from <http://www.msha.gov/alerts/hazardsofacetylene.htm> on 9 June 2016.

Muthukumar, G. and Kumar, M. (2015) 'Influence of openings on the structural response of shear wall', *Advances in Structural Engineering: Materials, Volume Three*, 2014, pp. 2229–2239. doi: 10.1007/978-81-322-2187-6\_169.

NCMA, N. C. M. A. (2014) 'Design of Concrete Masonry Walls for Blast Loading', *Tek 14-21a*, pp. 1–9.

Nyström, U. and Gylltoft, K. (2009) 'Numerical studies of the combined effects of blast and fragment loading', *International Journal of Impact Engineering*, 36(8), pp. 995–1005. doi: 10.1016/j.ijimpeng.2009.02.008.

Palanivelu, S., Paepegem, W. V., Degrieck, J., Reymen, B., Ndambi, J. M., Vantomme, J., Kakogiannis, D., Wastiels, J., Hemelrijck, D. V. (2011) 'Close-range blast loading on empty recyclable metal beverage cans for use in sacrificial cladding structure', *Engineering Structures*, 33(6), pp. 1966–1987. doi: 10.1016/j.engstruct.2011.02.034.

Rajan, S. P. (2018) 'Simulation of Building Demolition using ANSYS', *International Journal for Research in Applied Science and Engineering Technology*, 6(6), pp. 452–457. doi: 10.22214/ijraset.2018.6070.

Remennikov, A., Mentus, I. and Uy, B. (2015) 'Explosive Breaching of Walls with Contact Charges: Theory and Applications', *International Journal of Protective Structures*, 6(4), pp. 629–647. doi: 10.1260/2041-4196.6.4.629.

Rodriguez-Nikl, T., Hegemier, G. A. and Seible, F. (2011) 'Blast simulator testing of structures: Methodology and validation', *Shock and Vibration*, 18(4), pp. 579–592. doi: 10.3233/SAV-2010-0563.

Rouse, N. (2012) 'The Mitigation Effects of a Barrier Wall on Blast Wave Pressures', *International Society of Explosive Engineers*, pp. 1–8.

Seman, M. A., Syed Mohsin, S. M. and Jaini, Z. M. (2019) 'Blast Load Assessment: RC Wall Subjected to Blast Load', *IOP Conference Series: Earth and Environmental Science*, 244(1). doi: 10.1088/1755-1315/244/1/012007.

Stewart, L. K., Friedenber, A., Rodriguez Nikl, T., Oesterle, M., Wolfson, J., Durant, B., Arnett, K., Asaro, R. J., Hegemier, G. A. (2014) 'Methodology and validation for blast and shock testing of structures using high-speed hydraulic actuators', *Engineering Structures*, 70, pp. 168–180. doi: 10.1016/j.engstruct.2014.03.027.

Yang, S., Chegnizadeh, A. and Nikraz, H. (2013) 'Review of Studies on Retaining Wall's Behavior on Dynamic / Seismic Condition', *Int. Journal of Engineering Research and Applications*, 3(6), pp. 1012–1021. doi: 10.1128/AEM.72.1.769.

Yusof, M. A., Rosdi, R. N., Mohamad Nor, N., Ismail, A., Yahya, M. A., Peng, C. P. (2014) 'Simulation Of Reinforced Concrete Blast Wall Subjected To Air Blast Loading(3D concrete wall)', *Journal of Asian Scientific Research*, 4(49), pp. 522–533. Available at: <http://www.aessweb.com/journals/5003>.